Compensator Ground Fault Coverage Through a Delta-Wye Transformer – A Case Study

Dustin Hohenbery
Caterpillar

Ryan McDaniel, Harish Chaluvadi, and Michael J. Thompson
Schweitzer Engineering Laboratories, Inc.

Presented at the
73rd Annual Georgia Tech Protective Relaying Conference
Atlanta, Georgia
May 1–3, 2019

Originally presented at the
72nd Annual Conference for Protective Relay Engineers, March 2019

Compensator Ground Fault Coverage Through a Delta-Wye Transformer – A Case Study

Dustin Hohenbery, *Caterpillar*
Ryan McDaniel, Harish Chaluvadi, and Michael J. Thompson, *Schweitzer Engineering Laboratories, Inc.*

***Abstract*—Compensator distance protection is commonly used to protect transmission lines that have a delta-wye transformer between the relay location and protected line. The compensator element is unaffected by the phase shift of the transformer for faults.**

This paper includes results from a study on an in-zone ground fault on the high side of a wye-delta transformer for which the compensator element did not operate. A similarly set phase mho element did trip for this fault. To compare the fault coverage of each element, the characteristic plot of each element is shown for this fault.

I. Introduction

Distance relays are commonly applied on the low-voltage side of delta-wye transformers in looped systems to see faults on the high-voltage side of the transformers and trip a low-voltage-side breaker. This is typically done as a cost-saving measure because it is expensive to install high-voltage potential transformers (PTs) and a high-side transformer breaker. However, measuring an accurate impedance to the fault with a 30-degree phase shift in sequence quantities between the relay and the fault is challenging. Typically, in applications with transformers in-series of the protected line, protection engineers are concerned with selecting a distance element principle that can accurately measure impedance to the fault for phase-to-phase (PP), phase-to-phase-to-ground (PPG), and three-phase (3PH) faults. If set correctly, the compensator distance relay provides adequate performance for these fault types through a delta-wye transformer. Mho elements can also provide adequate protection for these fault types, but only if the relay has been designed, or uses special voltage transformer (VT) and current transformer (CT) connections, to reach through a transformer.

Generally, the performance of either distance relay type for phase-to-ground (PG) faults through a delta-wye transformer is not evaluated. Protection engineers do not expect coordination issues to develop because phase-distance elements have very limited response for PG faults. This is because the fault currents and voltages are affected by the zero-sequence network of the system; however, the relay observing the fault does not have access to zero-sequence voltage and current.

In this paper we will provide a case study from a real-world event in which phase-distance relays produced unexpected results for a fault involving ground through a delta-wye transformer. Further, we will provide a review and summary of phase element distance performances for various fault types.

II. Case Study

A. System Overview

The system studied is a manufacturing facility fed from two utility 34.5 kV overhead subtransmission lines as shown in Fig. 1. Each of the utility's 34.5 kV sources is stepped down by 34.5/13.2 kV, 9 megavolt ampere (MVA) delta-wye transformers. The distribution system at the facility is supplied by 13.2 kV Switchgear A and B and is operated with the bus-tie breaker closed for reliability of service. By operating with the bus-tie closed, the facility will continue to be supplied by one utility source in the event that the other source trips. The 13.2 kV feeders supply downstream unit substations, where the voltage is further stepped down to either 4160 V or 480 V, depending on the plant process requirements. For simplicity, only two feeders on each bus are shown in the figure.

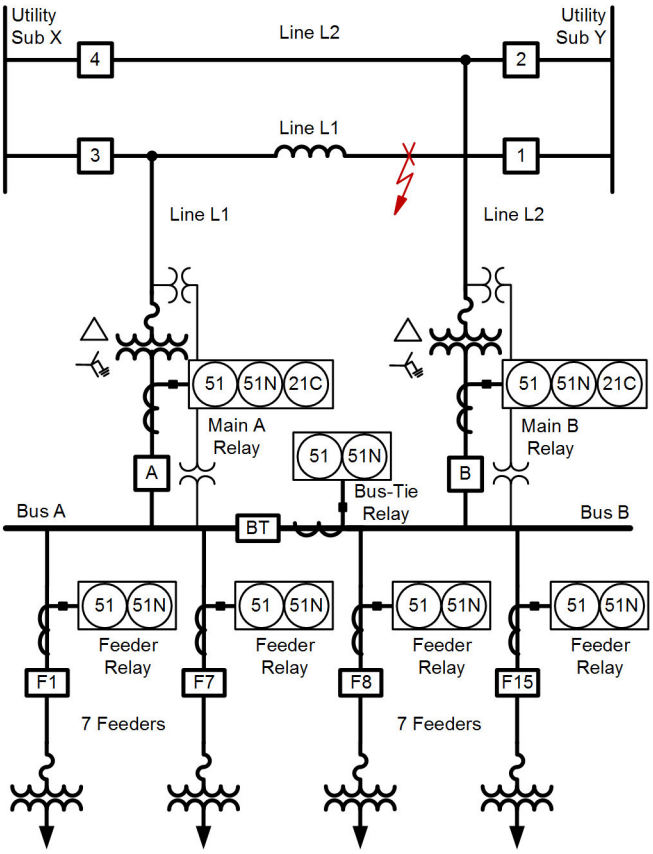

Fig. 1. Case Study Power System

The original switchgear was protected by electromechanical relays. The vintage switchgear was replaced with arc-resistant

switchgear as a part of an upgrade project. The new switchgear had multifunctional microprocessor-based relays to protect the feeders and the mains. For this case study, we will focus on the backfeed protection implemented at the manufacturing facility because it is germane to our event analysis

B. Backfeed Protection

The interconnecting utility requires backfeed protection when there is onsite generation or the commercial facility operates with the bus-tie closed. The intent of the backfeed protection is to prevent fault current from flowing into a fault on one service feeder through the other service feeders and the closed tie.

Various methods can be used for protection, such as sensitive reverse directional overcurrent elements [1] or reverse-looking distance elements.

At this facility there are two protection functions for isolating utility faults:

- Phase compensator distance protection
- Undervoltage (UV) and overvoltage (OV) protection scheme

An overreaching phase compensator distance element set directionally (reverse) toward the utility was selected instead of a traditional mho-type element because it provides better coverage for phase faults for lines with in-line transformers [2]. Moreover, the switchgear was designed with open-delta bus PTs. The relay model installed in the switchgear only supports compensator distance elements when open-delta PTs are connected because this type of element operates based only on positive- and negative-sequence quantities.

Two zones of protection are used. The transformer impedance is 2.96 ohms and the Line L1 impedance is 7.2 ohms. The instantaneous Zone 1 covers 80 percent of the transformer impedance. The 30-cycle time-delayed zone is typically set to 150 percent of the sum of the transformer and the 34.5 kV subtransmission feeder impedance. However, in this case the maximum allowable reach was selected in the relay to ensure the main tripped before the tie for any fault on the utility system.

The UV/OV scheme provides backup isolation of the mains. A PT on the 34.5 kV side of the transformer senses the utility voltage. The UV element is set to trip in 30 cycles when the voltage drops below 45 percent of nominal voltage. If a single-line-to-ground (SLG) fault is isolated from the utility side prior to the main opening, an overvoltage will occur on the unfaulted phases. The OV element would respond to such a situation and is set to 110 percent of nominal line-to-neutral voltage.

C. Event Summary

On December 29, 2017, a ground fault occurred on Line L1 of the utility system (Fig. 1) and led to an undesired operation of the relay at Breaker BT, dropping the Bus A load.

The ground overcurrent element (51GT) at Breaker 1 times out and trips Breaker 1 as expected, and is shown in the event report in Fig. 2. The figure shows that the current envelope of Phase C changed as the event continued. In the lower section of Fig. 2, we plot the apparent reactance (XLIM) and apparent resistance (RLIM) are plotted for the fault using (3) and (4) in [3]. Although the apparent reactance is unchanged, the apparent resistance varies between approximately 1 ohm and 2 ohms secondary during the fault.

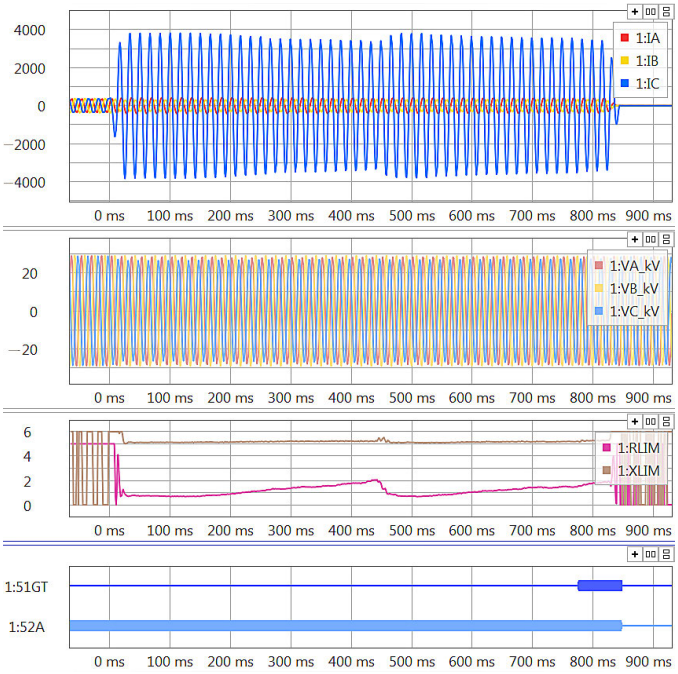

Fig. 2. Oscillography Record for Breaker 1

Breaker 3 is expected to also open for this fault; however, no event data were available from Breaker 3. It is possible that Breaker 3 was already open prior to the fault, and the ground fault was sustained by shunt loads on Line L1. This possibility will be discussed more in Section IV.

The next event report we inspect is from Main A Breaker, which is supposed to coordinate with the overcurrent relaying on Breaker BT for utility faults. Fig. 3 shows the oscillography from Main A Breaker.

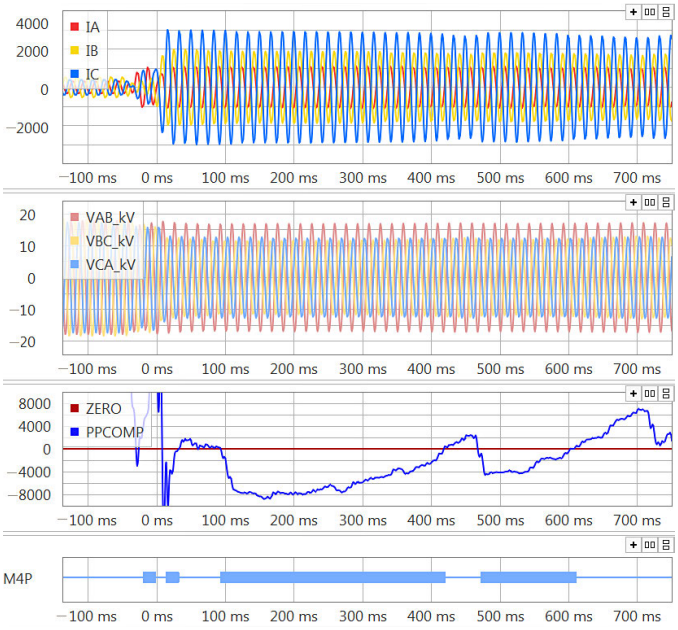

Fig. 3. Oscillography Record for Main A Breaker

The word bit M4P asserts when the compensator relay declares the fault within the zone of protection. It did not stay solidly asserted. To validate this performance, we also plot the torque evaluation of the phase-to-phase compensator unit (PPCOMP) using Equations (1) and (2).

$$S1_{PPCOMP} = V_{AB} - I_{AB} \bullet Z1_R$$
$$S2_{PPCOMP} = V_{BC} - I_{BC} \bullet Z1_R \quad (1)$$

$$PPCOMP_{TORQUE} = IM(S1 \bullet S2^*) \quad (2)$$

A negative torque produces an operate condition; whereas, a positive torque produces a restrain condition. We see that the torque evaluation lines up well with the M4P word bit. We also note that the torque of the PPCOMP relay appears to have a correlation with the fault resistance shown in Fig. 2. As the fault resistance decreases, the PPCOMP torque tends toward an operate condition. This is most apparent between the 400 milliseconds (ms) and 500 ms mark in each event, when both the resistance and torque sharply drop.

Because the PPCOMP relay was not able to stay solidly asserted, it never times out after 30 cycles as was intended. If it had, the facility would have been isolated from the fault and no load would have been lost. The tie breaker, which saw about the same magnitude of IC current as the Breaker A relay (about 5 amperes secondary), began timing on a 51 element with a pickup set at 2 amperes secondary. After approximately 1.8 seconds, the bus-tie breaker opened to isolate the facility from the fault.

This situation could have been avoided had either of these things happened:

1. Main Breaker A tripped on the time-delayed compensator distance element
2. Main Breaker A tripped on UV/OV scheme

D. Initial Compensator Distance Analysis

The manufacturing facility wanted to find a way to improve the performance of the Breaker A relays for this fault. Because the compensator relay at Breaker A was already set to its maximum reach (64 ohms), it did not seem as if more dependability could be gained. However, we found that pulling the reach back began to lead to increased dependability for this fault.

We picked a moment in the fault in which the PPCOMP relay underreached the most (highest positive torque) and then altered the reach setting to observe how the torque changed. The results are shown in Fig. 4.

The results from Fig. 4 are perplexing. We found that relay reach settings between 12 and 58 ohms would lead to dependability for this fault. However, increasing the relay reach setting above 58 ohms leads to less dependability.

We then evaluated self-polarized phase-to-phase mho element (MHO(PP)) torques for reaches from 0 to 64 ohms using (3) and (4).

$$S1_{PPMHO(SELF)} = V_{pp} - I_{pp} \bullet Z1_R$$
$$S2_{PPMHO(SELF)} = V_{pp} \quad (3)$$

$$PPMHO(SELF)_{TORQUE} = RE(S1 \bullet S2^*) \quad (4)$$

Again, a torque that evaluates negative is an operate condition.

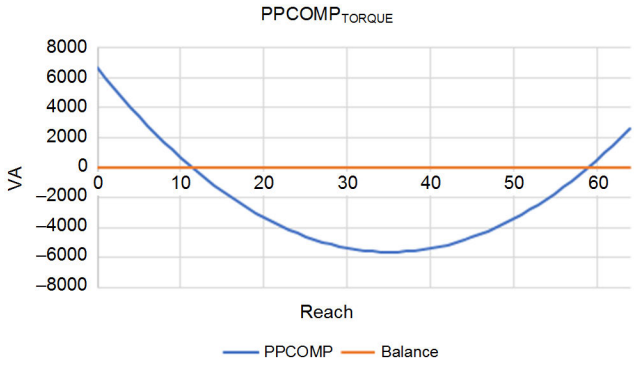

Fig. 4. $PPCOMP_{TORQUE}$ for Relay Reaches 0 to 64 Ohms

The results of the torque evaluation are shown in Fig. 5.

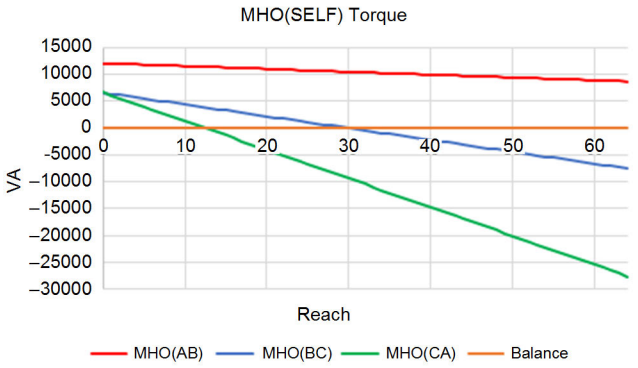

Fig. 5. Mho Torque for Relay Reaches 0 to 64 Ohms

The results from Fig. 5 are more aligned with what we expect: As we increase the relay reach, we increase the torque in the negative (operate) direction. We find that a reach of 12 ohms or greater using a self-polarized PP mho would have led to an operation for this fault. MHO(CA) was the best-performing element for this fault.

Plotting the toque evaluation for the PPCOMP relay leads us to the question: Why does increasing the reach decrease the dependability for this fault?

III. Plotting Dynamic Compensator Characteristic

To understand the unexpected behavior of the compensator element, we need a way to visualize how extending the relay reach can lead to less dependability. In [4], author Don Fentie describes how to plot a dynamic characteristic of the mho element by finding the center and radius of a mho circle based on relay input quantities. We want to plot the dynamic characteristic of the compensator element, which means we must also find the center and radius of the characteristic circle based on relay input quantities.

A. Review Static Compensator Characteristic

The compensator distance relay was originally explained by W. K. Sonnemann [5] and is also discussed in [6]. The original compensator distance relay is made up of two separate relays:

1. Three-phase relay (3PCOMP) designed to detect 3PH faults and provide coverage for close-in PPG faults in systems with a low source impedance
2. PP relay (PPCOMP) designed to detect all PP faults and most PPG faults

We turn our attention to the PPCOMP relay, for which the torque analysis was provided in Section II. Sonneman derives the operating characteristic for the PPCOMP unit for PP faults in [5]. This derivation is only applicable for no-load conditions; however, it is a good starting point to define the dynamic PPCOMP characteristic. The key takeaway from the derivation is that the PPCOMP relay balances the ratio of V1/V2 at the relay reach point ($Z1_R$) as shown in (5).

$$\frac{V1_R - I1_R \bullet Z1_R}{V2_R - I2_R \bullet Z1_R} = 1\angle\theta \tag{5}$$

Reference [6] defines the numerator of (5) as the line-drop-compensated V1 (V1C) and the denominator of (5) as the line-drop-compensated V2 (V2C). If V2C exceeds V1C, then the fault must be inside the relay reach, therefore an operate condition. Expressed another way, if |V1C/V2C| is less than 1 at the relay reach point, then it is an operate condition. The inherent advantage to this design is that the relay is unaffected by phase shifts in the positive- and negative-sequence networks because of delta-wye transformers.

To define the dynamic PPCOMP characteristic, we start with (5) and define $V1_R$ and $I1_R$ to include the effects of loading.

B. Dynamic Compensator Characteristic

Fig. 6 shows the sequence network connections for a bolted (no arc resistance) PP fault and the pre-fault positive-sequence network. In these and subsequent figures, the pennant symbol represents the location at which the relay is observing the power system network. Because the PPCOMP only responds to positive- and negative-sequence networks, this fault type will be the easiest for us to define the characteristic.

The pre-fault network is an ideal two-machine system with sending voltage (ES) and receiving voltage (ER). If there is a difference in the two voltages, current will be flowing prior to the fault, which we define as $I1_R pf$. From this pre-fault current, we will calculate a voltage (ETH) that defines the available voltage at the fault point. Using the principle of superposition, we use this ETH voltage as the source in the pure-fault network. We can then solve for the pure-fault currents ($\Delta I1_R$ and $I2_R$) and the pure-fault voltages ($\Delta V1_R$ and $V2_R$). These values are then used to find the fault network relay voltages ($V1_R$ and $V2_R$) and fault network relay currents ($I1_R$ and $I2_R$) using (3) from [7], as shown in (6).

$$\begin{aligned} V1_R &= V1_R pf + \Delta V1_R \\ I1_R &= I1_R pf + \Delta I1_R \end{aligned} \tag{6}$$

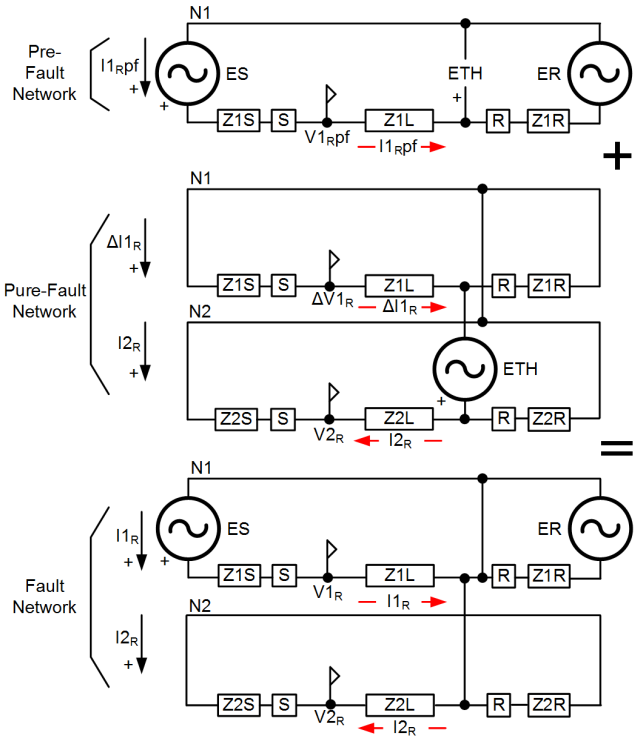

Fig. 6. Sequence Networks for PP Fault

As shown in Fig. 6, note that Z1S is the Thévenin equivalent positive-sequence impedance of the sending source (ES) and Z1R is the Thévenin equivalent positive-sequence impedance of the receiving source (ER). Z1L is the positive-sequence impedance starting from the relay location and ending at the fault point. Ultimately, we want to define Z1L in terms of quantities known to the relay, which means any information from the remote source is unavailable to us.

From Fig. 6, our goal is to define $V1_R$, $I1_R$, $V2_R$, and $I2_R$ so we can simplify (5). First, we start with defining $V1_R$.

From analysis of the Fig. 6 pure-fault network, we can define $\Delta V1_R$ in terms of the negative-sequence current, which will help when simplifying (5):

$$\Delta V1_R = -I2_R \bullet (Z1S + 2 \bullet Z1L) - ETH \tag{7}$$

We define $V1_R pf$:

$$V1_R pf = (ETH + I1_R pf \bullet Z1L) \tag{8}$$

The result for V1R using (6) is shown in (9)

$$V1_R = I1_R pf \bullet Z1L - I2_R \bullet (Z1S + 2 \bullet Z1L) \tag{9}$$

Next we define $I1_R$. We can recognize from the Fig. 6 pure-fault network that $\Delta I1_R = -I2_R$, which leads to (10).

$$I1_R = I1_R pf - I2_R \tag{10}$$

Lastly, we define $V2_R$ in terms of $I2_R$:

$$V2_R = -I2_R \bullet Z1S \tag{11}$$

Taking the definitions from (9), (10), and (11), we apply them to (5) and get (12):

$$1\angle\theta = \frac{(I1_R pf \bullet Z1L - I2_R \bullet (Z1S + 2 \bullet Z1L))}{-(I1_R pf - I2_R) \bullet Z1_R} \tag{12}$$
$$-I2_R \bullet Z1S - I2_R \bullet Z1_R$$

We can then solve (12) for ZIL and reduce to (13):

$$Z1L = 1\angle\theta \bullet \left(\frac{(Z1S + Z1_R)}{\left(2 + \frac{I1_R pf}{-I2_R}\right)} \right) + \frac{-Z1S + Z1_R \bullet \left(1 + \frac{I1_R pf}{-I2_R}\right)}{\left(2 + \frac{I1_R pf}{-I2_R}\right)} \tag{13}$$

Equation (13) is similar in form to the static compensator plot given by Sonneman [5], except this derivation includes pre-fault load, and therefore can be used to plot the dynamic characteristic of the PPCOMP relay. In fact, if $I1_R pf = 0$, then (13) exactly matches the derivation in [5]. The center of the circle is defined by the second term in (13).

$$\text{Center} = \frac{-Z1S + Z1_R \bullet \left(1 + \frac{I1_R pf}{-I2_R}\right)}{\left(2 + \frac{I1_R pf}{-I2_R}\right)} \tag{14}$$

The radius of the circle is defined by the first term of (13):

$$\text{Radius} = \text{abs}\left(\frac{(Z1S + Z1_R)}{(2 + \frac{I1_R pf}{-I2_R})} \right) \tag{15}$$

The Z1S term is defined by V2 and I2 as shown in (11). Therefore, the relay will have access to all required quantities.

To plot the characteristic, a software tool capable of simulating a two-source system and plotting circles was selected. In addition, a positive-sequence memory-polarized mho element was plotted for comparison purposes using the equations in [4]. Fig. 7 shows the result for a BC fault at the Z1L point in a system in which Z1S, Z1L, and Z1R = 1 ∠90. The relay reach of $Z1_R$ is also set to 1 ∠90. The plot on the left shows a no-load flow condition (σ = 0, ES = 1∠0 and ER = 1 ∠0) and the $MHO(BC)_{MEM}$ and PPCOMP are exactly the same. The plot on the right shows a forward-load flow condition (σ=30, ES = 1 ∠30, and ER = 1∠0). We can see that the PPCOMP characteristic shifts to the left more than the $MHO(BC)_{MEM}$. This reduces the arc-resistance coverage of the PPCOMP compared to the $MHO(BC)_{MEM}$ for forward-load flows. The topic of arc-resistance coverage during loading conditions for the PPCOMP relay is covered in [8]. Also, it is interesting to note that the PPCOMP characteristic provides a circle expansion back to the source (Z1S) without the need for memory.

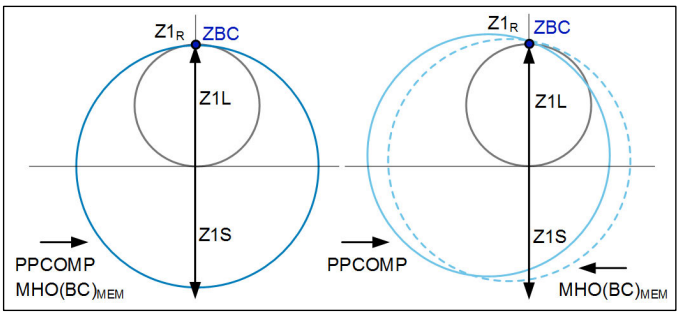

Fig. 7. PPCOMP and $MHO(BC)_{MEM}$ for No-Load Flow (Left), and Forward-Load Flow (Right)

While the PPCOMP relay is a multiple-phase relay designed to detect all PP faults, its characteristic can be represented in terms of ZAB, ZBC, and ZCA by changing the reference phase used in calculating symmetrical components. In Fig. 7, we are plotting a BC fault and the symmetrical components are referenced to Phase A. If we were looking at a CA fault and wanted to compare the compensator to the ZCA loop impedance, we would use Phase B as our symmetrical component reference in (13). Regardless of which symmetrical component reference is used to plot the characteristic, the performance of the PPCOMP relay is the same.

Now that we have defined the dynamic compensator characteristic, we want to look at how a delta-wye transformer effects the impedance loop measurements of distance relays.

IV. Transformer Connection Effects on Distance Elements for Standard Fault Types

Distance relays use fault-loop voltages and currents to measure an apparent fault-loop impedance to the fault. A delta-wye or wye-delta transformer between the relay and the fault will produce a phase shift between the positive- and negative-sequence currents, which will affect the fault-loop impedance measurements. The fault loops that we measure can be broken into two basic categories: PP fault loops (AB, BC, and CA) and ground-fault loops (AG, BG, and CG). The general formula for PP fault-loop impedance is given in (16); whereas, the PG fault-loop impedance is given in (17).

$$Z\phi\phi = \frac{V\phi\phi}{I\phi\phi} \tag{16}$$

$$Z\phi G = \frac{V\phi G}{I\phi + 3 \bullet I0 \bullet \frac{Z0 - Z1}{3 \bullet Z1}} \tag{17}$$

How are these loops affected by a delta-wye or wye-delta transformer between the relay and the fault?

Throughout this paper, we will ignore the influence that auxiliary distance relay logic (such as fault identification logic) [9] would have on influencing whether certain phase or ground loops are released and allowed to trip. We simply look at whether the fault-loop impedance plots within the characteristics we are observing.

A. *Review Sequence Networks for Transformer Connections*

We will examine DY1 and DY11 transformers as well as YD1 and YD11 transformers. In these transformer designations, the number represents the multiple of 30 degrees for which the second winding lags the first winding. For example, a DY11 transformer has the wye winding lagging the delta winding by 330° (–30°). In this paper we do not use the convention of using a lower-case letter to indicate the secondary winding of the transformer. Because the focus of the paper is on what the relay measures looking through the transformer, the relay could be on either the low side or the high side. In the discussion, the side with the relay is the side designated by the first letter of the transformer designation.

For simplicity, we will assume an infinite source connected to the side of the transformer where the relay is located. The transformer has a Z1 and Z0 per unit (pu) impedance of 1 ∠90. Again for simplicity, the voltages on each side of the transformer have the same PP voltage rating. We will then show the phase voltages and currents and the sequence voltages and currents, as seen by the relay for faults on the opposite side of the transformer. We will examine all four fault types: PG, PP, PPG, and 3PH.

1) *DY1/DY11 Transformer – SLG Fault*

We will start with a common DY1 transformer. Fig. 8 shows the phase and sequence quantities that we will see on each side of the DY1 transformer for an AG fault on the wye side. What appears to be an AG fault on the wye side looks like a CA fault on the delta side.

The phasor diagram on the right (Fig. 8 Box 2) shows the phase voltages and currents for this Phase A-to-ground fault. The DY1 transformer will shift the delta side positive-sequence voltages and currents by +30 degrees and shift the negative-sequence voltages and currents by –30 degrees relative to the wye side. There are no zero-sequence quantities available on the delta side. This relationship will remain the same for the subsequent fault types that we analyze.

In Fig. 8 Box 1, we rotate the delta-side phasors so that V1H is the reference. We then see that we can simply shift the negative-sequence voltages and currents by –60 degrees and leave the positive-sequence network unaffected. This serves us well because it will allow us to unclutter the positive-sequence network and easily simulate load conditions if we so choose. We note that because we are assuming an infinite source, there is no V2H present. However, we show it as a dotted line to indicate what would happen as the source increased. We did not show shifting of the wye-side phasors in Box 1 of Fig. 8 to match the shift of the delta-side phasors because we are not concerned with those quantities in this paper. However, it is important to note that if a V1H reference is shifted, the wye-side phasors must also be shifted, if they are intended to be used in analyses. This is particularly important if analyzing differential currents.

From the previous discussion, it should be evident that a DY11 transformer would be similar to a DY1 transformer, except the phase shift in the negative-sequence network would be +60 degrees. Additionally, the AG fault would appear to be an AB fault instead of a CA fault on the delta side of the transformer.

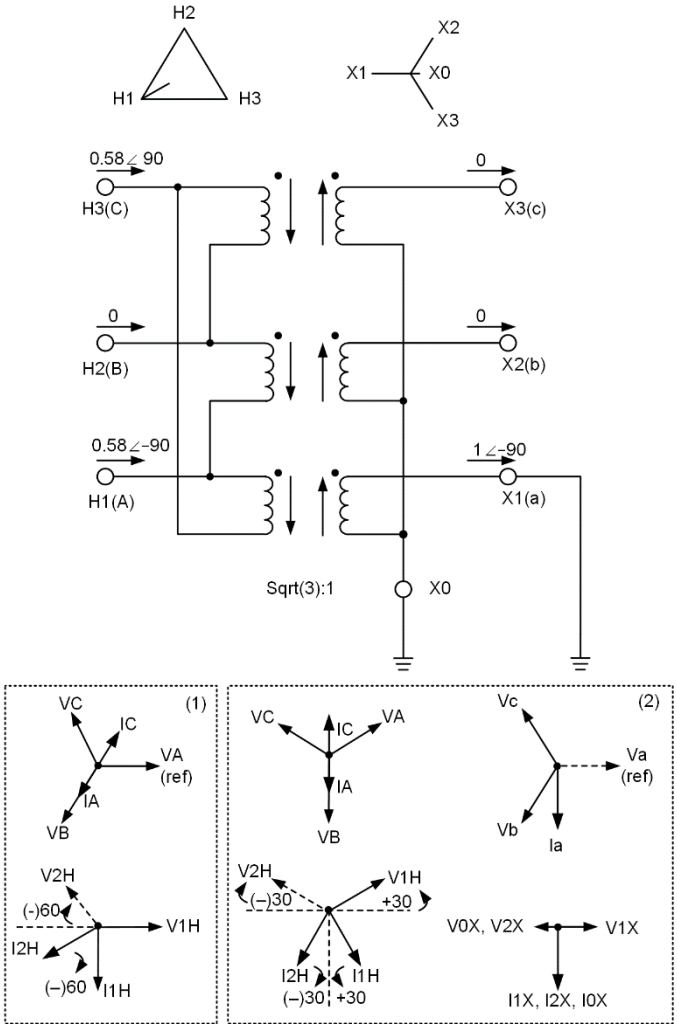

Fig. 8. DY1 Transformer – Wye-Side AG Fault

From this discussion, we can define the sequence network connections when analyzing PG faults through a delta-wye transformer in a two-source system, which is shown in Fig. 9.

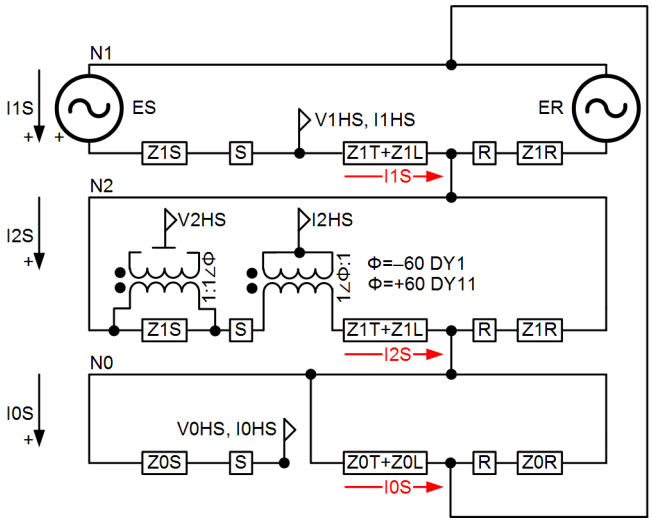

Fig. 9. Sequence Network Connections for Phase-to-Ground Fault Through Delta-Wye Transformer

To get an idea of the effects of the phase shift introduced by a DY1 and a DY11 transformer for a Phase A-to-ground fault, we plot the excited fault-loop impedances in the complex impedance plane with the mho and PPCOMP characteristics. The system parameters used for this fault and subsequent faults in the section are Z1S = Z0S = 0 and Z1T + Z1L = Z0T + Z0L = Z1R = Z0R = 1∠90. The distance element reach, $Z1_R$, is set at 1∠90.

First we start with a Phase A-to-ground fault, but without the phase shift introduced by the transformer. This is shown in Fig. 10.

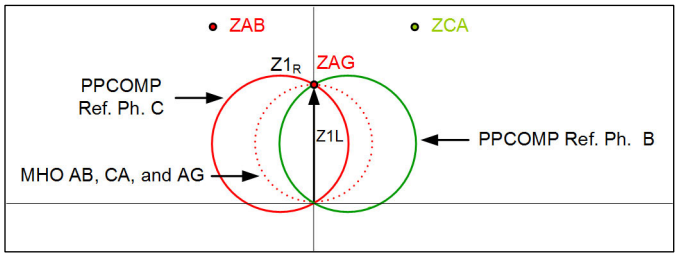

Fig. 10. Measured Fault-Loop Impedances Without Transformer for AG Fault

The red-dashed circle in Fig. 10 represents the characteristic of all the mho elements that respond to this AG fault (AB, CA, and AG). The green circle represents the PPCOMP, referenced to Phase B symmetrical components, and the solid red circle represents the PPCOMP, referenced to Phase C symmetrical components. As previously discussed, each phase loop will respond the same regarding the PPCOMP; we can graphically see this because the green circle is the same distance from ZCA as the red circle is from ZAB. For the remainder of the paper, we will only plot the PPCOMP characteristic for the best-performing mho fault loop.

We see that ZAG perfectly represents the impedance to the fault for a Phase AG fault with no transformer between the relay and the fault. The AB and CA loops are excited; however, the apparent impedance of those loops is well outside the reach of the plotted relay characteristics. Interestingly, the PPCOMP responds a bit better than the MHO(AB) and MHO(CA) relays for a Phase-A PG fault; however, it still underreaches significantly. We can see that the PPCOMP characteristic shifts toward the fault loop to which it is referenced.

When the transformer is introduced for the same fault type (Fig. 11 and Fig. 12), more fault loops are excited; however, none of them accurately measure the expected impedance between the relay and the fault. The circle in Fig. 11 represents all mho elements excited for this AG fault as well as the PPCOMP element referenced to the ZCA impedance through a DY1 transformer. Because this looks like a CA fault, any fault loop involving C or A will respond. Only the BG loop will not see fault current.

In Fig. 11, the best-performing phase mho, MHO(CA), underreaches for a fault through a DY1 transformer by a factor of 0.67. We can explain this by looking at (16) and recognizing that the numerator will evaluate to a magnitude of √3 pu (1 ∠120 – 1 ∠0). The currents in the denominator will evaluate to a magnitude of 2 / √3 pu (1 / √3 ∠60 – 1 / √3 ∠–120). By dividing the magnitudes, we arrive at 3 / 2 = 1.5. The resultant angle of ZCA is 90 degrees. Therefore, a phase loop would need to be set at 1.5 times the expected reach to operate.

In Fig. 12, the circle represents all mho elements excited for this AG fault, as well as PPCOMP referenced to the ZAB impedance through a DY11 transformer. Because this looks like an AB fault, any fault loop involving A or B will respond. The MHO(AB) relay will underreach by a factor of 0.67. Only the CG loop will not see fault current. The PPCOMP relay performs the same as a MHO(PP) relay for SLG faults through a delta-wye transformer.

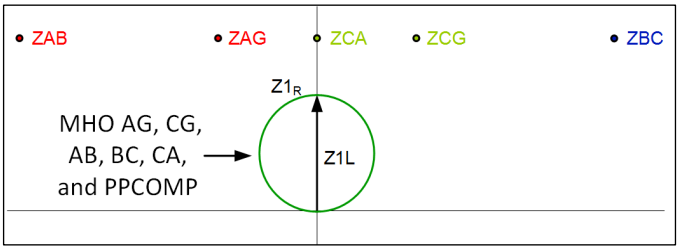

Fig. 11. Measured Fault-Loop Impedances with DY1 Transformer for AG Fault

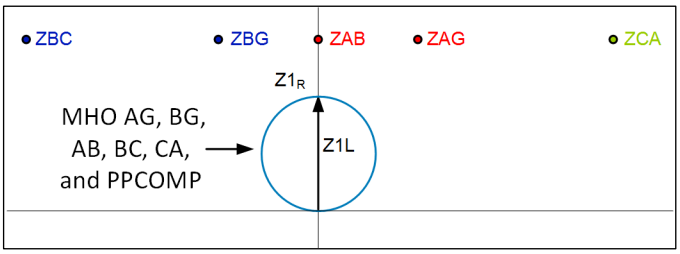

Fig. 12. Measured Fault-Loop Impedances with DY11 Transformer for AG Fault

Next, we want to see what effect varying source parameters has on altering the loop impedances for a PG fault through a DY1 transformer. If the loop impedances vary for changing ZS and ZR parameters, then a distance relay has no benefit over a directional overcurrent relay. Fig. 13 shows how the ZCA impedance varies and Fig. 14 shows how the ZAG and ZCG impedance varies as the ZS and ZR changes. Of course, the ground elements would not normally be released in this case because of the lack of 3I0 measured by the relay. When varying ZS, ZR was kept at 1 ohm. When varying ZR, ZS was kept at 1 ohm. For all cases, the Z1 = Z0.

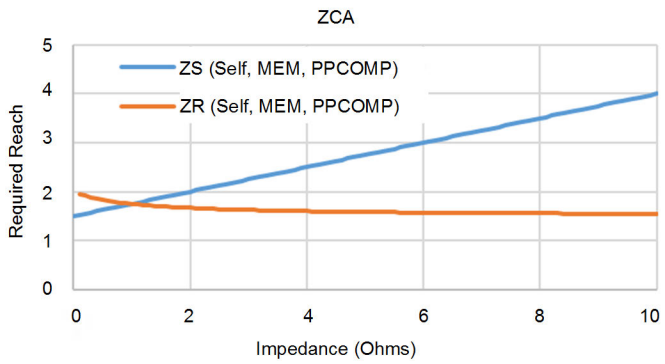

Fig. 13. Reach Required to See 1 Ohm Fault With Varying Source Impedances in DY1 Transformer

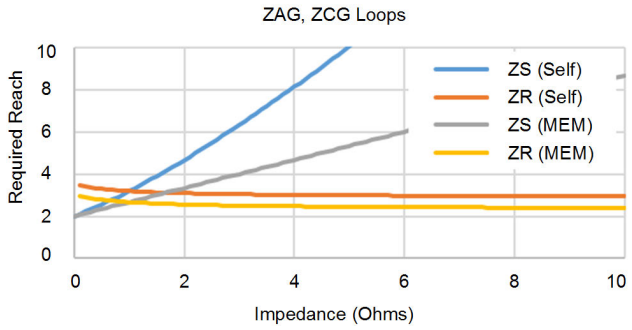

Fig. 14. Reach Required to See 1 Ohm Fault With Varying Source Impedances in DY1 Transformer

Fig. 13 and Fig. 14 show that using a distance relay to adequately protect a line through a delta-wye transformer for PG faults is a futile effort. If the local source impedance, ZS, changes, the effective reach of the relay changes. The remote source, ZR, also has some effect on relay reach. Therefore, although it is possible to see PG faults with a distance relay on the opposite side of a delta-wye transformer, all considered distance relays will severely underreach.

We note that the PPCOMP relay responds exactly the same as a MHO(CA) relay for AG faults on the DY1 transformer under no-load conditions. There is no advantage for either relay regarding reaching through a delta-wye transformer for PG faults.

Lastly, we can see that memory polarization does influence reach with ground elements looking through a transformer. This is because the ground-loop impedance is not at the maximum torque angle of the distance element. The expanded size of the mho circle does produce some reach benefit.

2) YD1/YD11 Transformer – SLG Fault

Because the case study is based on this configuration, we also supply the sequence diagram for a wye-delta transformer (Fig. 15) because the zero-sequence network connection is different from a delta-wye connection. In this configuration, fault current can only flow if Breaker R is closed. In Section V, we will discuss how shunt loads on the protected line can offer a fault path, even if Breaker R is open.

In this configuration, the result of varying the remote source impedance, ZR, has a more dramatic impact on the effective reach of a distance relay as shown in Fig. 16 and Fig. 17. This is because there is no current divider in the zero-sequence network. All zero-sequence fault current flows through Z0R. These figures support the case for a YD1 transformer.

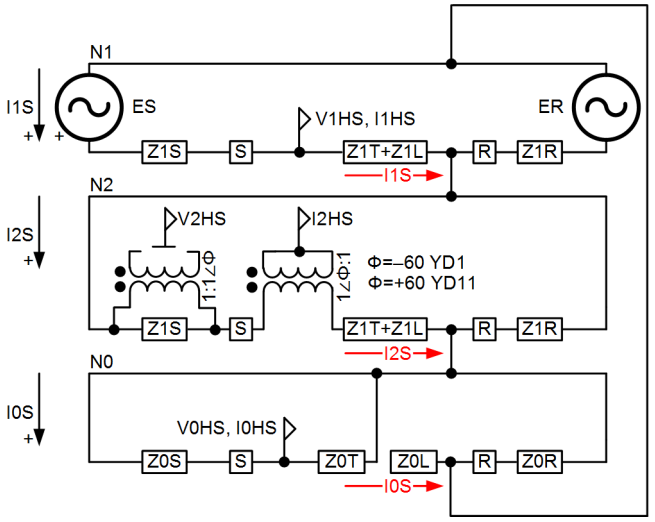

Fig. 15. Sequence Network Connections for Phase-to-Ground Fault Through Delta-Wye Transformer

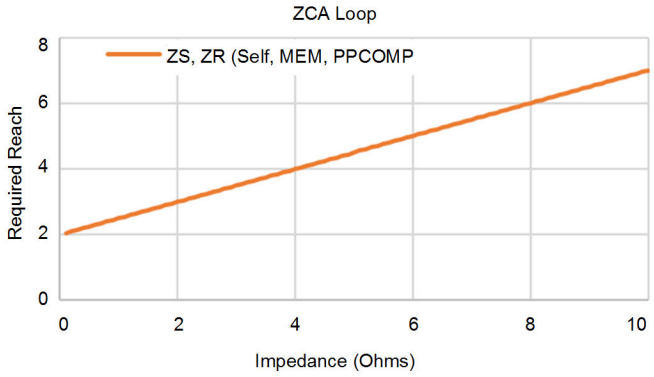

Fig. 16. Reach Required to See 1 Ohm Fault With Varying Source Impedances

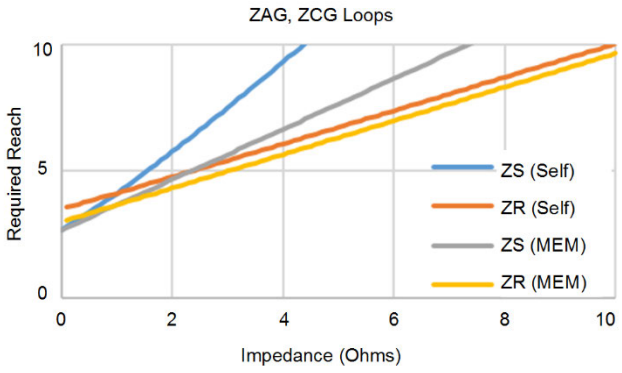

Fig. 17. Reach Required to See 1 Ohm Fault With Varying Source Impedances

3) DY1/DY11 Transformer – PP Fault

Fig. 18 shows the phase and sequence quantities we will see on each side of the DY1 transformer for a BC fault. What appears to be an BC fault on the wye side of the transformer looks unlike any standard fault type on the delta side of the transformer.

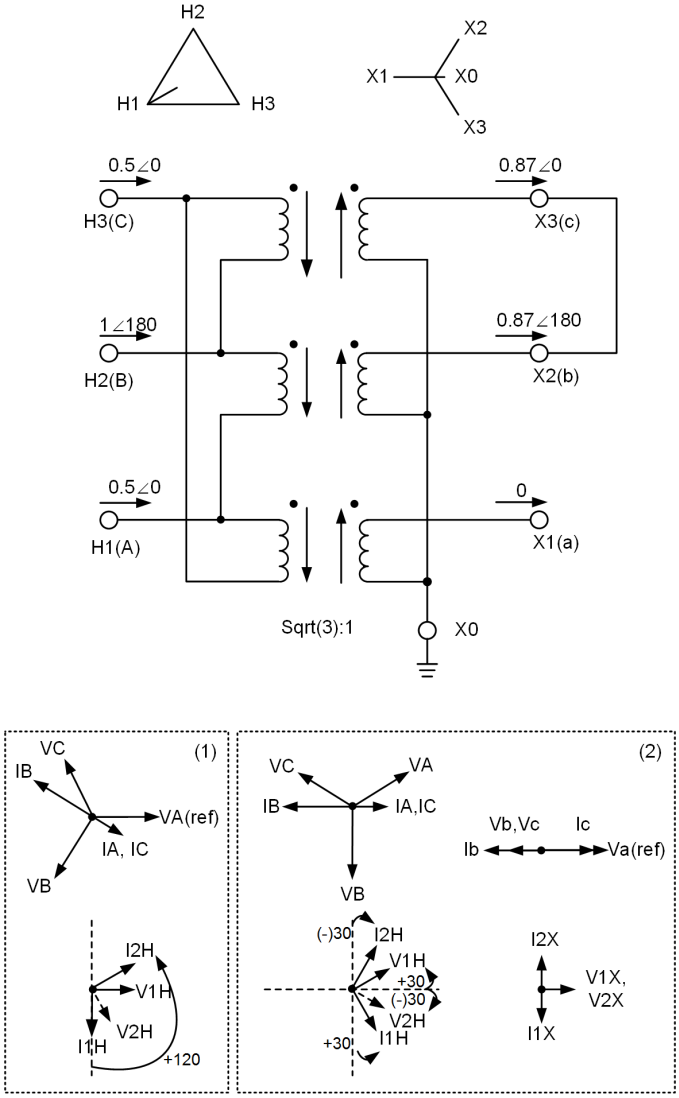

Fig. 18. DY1 Transformer – Wye-Side BC Fault

We can define the sequence network connections when analyzing PP faults through a delta-wye transformer in a two-source system (Fig. 19).

Using the same parameters as defined for the PG fault, we now evaluate the mho and the PPCOMP relay characteristic for a PP fault with and without the delta-wye transformer. We begin by starting with a BC fault, but without the phase shift introduced by the transformer. This is shown in Fig. 20.

In Fig. 20, the solid circle represents the characteristic of all mho elements that respond to this BC fault as well as the PPCOMP referenced to ZBC impedance. We see that ZBC perfectly represents the impedance to the fault for a Phase-BC fault with no transformer between the relay and the fault.

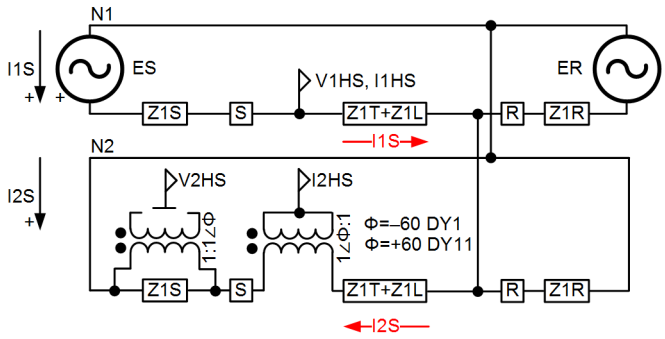

Fig. 19. Sequence Network Connections for Phase-to-Phase Fault Through Delta-Wye Transformer

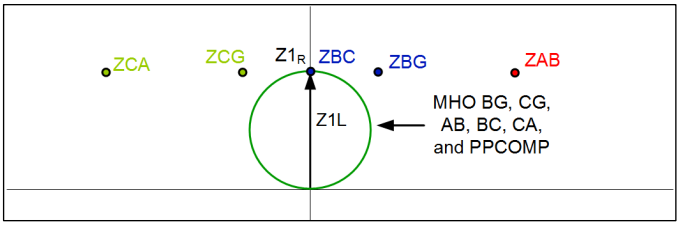

Fig. 20. Measured Fault-Loop Impedances Without Transformer for BC Fault

When the transformer is introduced for the same fault type (Fig. 21 and Fig. 22), we can see that the ZBC fault-loop impedance has shifted. The dashed circles in Fig. 21 and Fig. 22 represent all mho elements excited for this BC fault. The solid blue circles represent the PPCOMP referenced to ZBC impedance. The PPCOMP relay is unaffected by the shift in the ZBC fault-loop impedance. The ratio of V1C/V2C for the Phase BC fault at the reach point in each system configuration is as follows: V1C / V2C = 1 ∠0 (no transformer), V1C / V2C = 1 ∠60 (DY1 transformer), and V1C / V2C = 1 ∠–60 (DY11 transformer). In each case the |V1C / V2C| = 1; therefore, the relay is at its balance point. Conversely, a MHO(BC) relay, which operates specifically on the ZBC fault-loop impedance, will see the following ZBC values: 1 ∠90 pu (no transformer), 2 / √3 ∠120 pu (DY1 transformer), and 2 / √3 ∠60 pu (DY11 transformer). The MHO(PP) relay will underreach for PP faults through a transformer.

Interestingly, the ZBG fault-loop impedance is accurate for a BC fault through a DY1 transformer and the ZCG fault-loop impedance is accurate for a BC fault through a DY11 transformer. However, because the relay does not see 3I0, the ground loops would typically not be released.

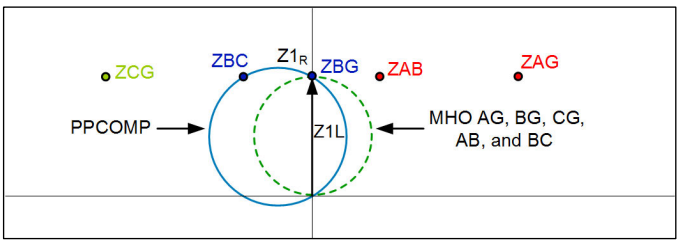

Fig. 21. Measured Fault-Loop Impedances With DY1 Transformer for a BC Fault

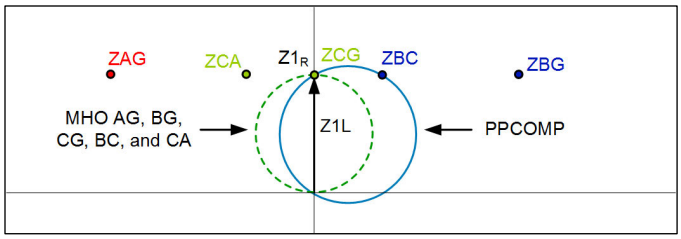

Fig. 22. Measured Fault-Loop Impedances With DY11 Transformer for BC Fault

Next we want to see what effect varying source parameters have on altering the loop impedances for a PP fault through a delta-wye transformer. Changes in remote source impedance, ZR, do not affect the mho element reach for PP faults. Fig. 23 shows how the phase-loop impedance varies as the local source impedance, ZS, changes. Fig. 24 shows how the ground-loop impedance varies. When varying ZS, ZR was kept at 1 ohm.

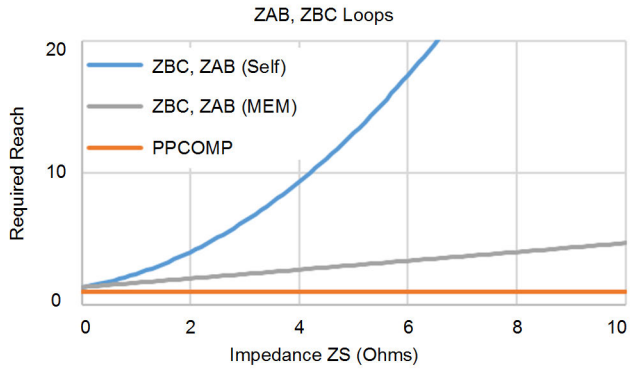

Fig. 23. Reach Required to See 1 Ohm Fault With Varying Source Impedances

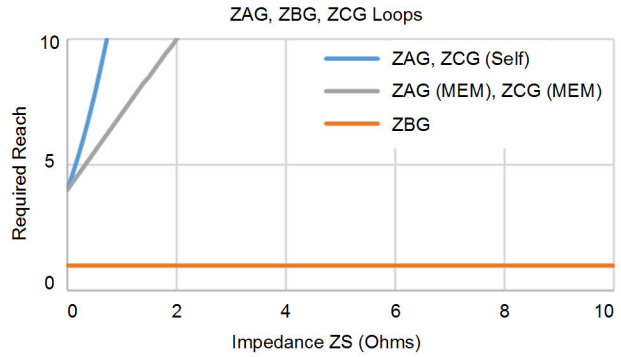

Fig. 24. Reach Required to See 1 Ohm Fault With Varying Source Impedances

4) Phase-Compensated Mho Element

The results from Fig. 23 and Fig. 24 show us that a PPCOMP relay and a MHO(BG) relay can be used to reach through a DY1 transformer to detect BC faults, which warrants further discussion.

While the compensator relay may be the more common method to reach through a transformer, some relays offer an option to use a MHO(PP) with compensation ($MHO(PP)_{COMP}$) to reach through a delta-wye transformer [10]. The idea of this compensation is to retrieve the AB, BC, and CA loops from the faulted side of the transformer, while taking into account the transformer connection and the quantities available to the relay on the unfaulted side.

To illustrate this, we assume our relay is on the wye side of a DY11 transformer, and we want to see the PP fault loops on the delta side. Fig. 25 shows a phasors diagram in which the wye-side phasors are represented in black, the delta-side phasors are represent in red, and the AB, BC, and CA loops on the delta side are represented in green.

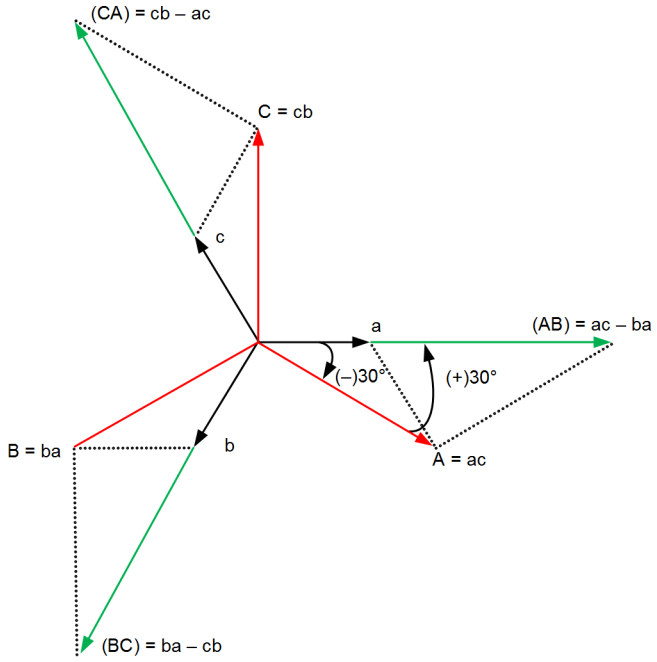

Fig. 25. AB, BC, and CA Loops on Delta Side of Transformer Referenced to the Wye Side (DY11)

We can see that for this transformer connection, there is a no phase shift between "a" and "(AB)." Conceptually, this should make some sense because the transformer connection is "ac" (–30) and the loop we want to see is "(AB)" (+30). We can see there are two ways to obtain the required quantities for the $MHO(AB)_{COMP}$ relay: use "a," or use (ab – ca)/3 (the division by three is needed to adjust for the increased magnitude). In practice, the $MHO(AB)_{COMP}$ uses Ia current and (Vab – Vca)/3 voltages. Because there is a break in the zero-sequence network between the relay location and the fault location, it is prudent to remove any standing zero-sequence voltage at the relay location because it has no bearing on the fault loops. However, zero-sequence removal is not used for the currents because zero-sequence current cannot flow through the transformer. The definitions for the correct fault loops follow. Note that the voltages have been reorganized from Fig. 25, but are equal.

Relay location leads fault-loop location by 30 degrees:

- $MHO(AB)_{COMP}$: V = (Vab – Vca) / 3, I = Ia
- $MHO(BC)_{COMP}$: V = (Vbc – Vab) / 3, I = Ib
- $MHO(CA)_{COMP}$: V = (Vca – Vbc) / 3, I = Ic

This explains why MHO(BG) performs well in Fig. 21. The relay location leads the fault-loop location by 30 degrees, and a BC fault was being simulated. If we assume there is no standing V0 at the relay location (ideal), there is no difference between $MHO(BC)_{COMP}$ and MHO(BG) for this fault.

Next, we assume our relay is on the wye side of a DY1 transformer, and we want to see the PP fault loops on the delta side of the transformer. Fig. 26 shows a phasors diagram using the same color scheme in Fig. 25.

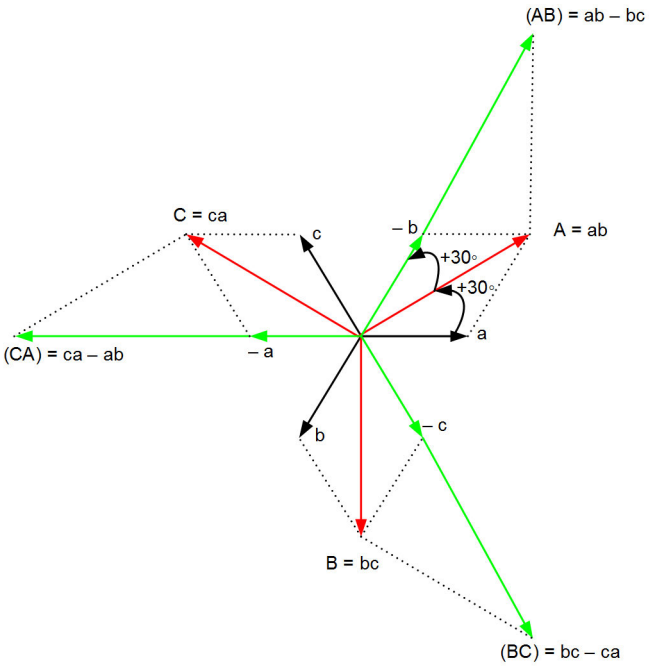

Fig. 26. AB, BC and CA Loops on Delta Side of Transformer Referenced to the Wye Side (DY1)

We can see that for this transformer connection, there is a 60 degree phase shift between "a" and "(AB)." Conceptually, this should make some sense as the transformer connection is "ab" (+30) and the loop we want to see is "(AB)" (another +30). We define the correct fault loops below.

Relay location lags fault-loop location by 30 degrees:

- MHO(AB)$_{COMP}$: V = (Vab – Vbc) / 3, I = –Ib
- MHO(BC)$_{COMP}$: V = (Vbc – Vca) / 3, I = –Ic
- MHO(CA)$_{COMP}$: V = (Vca – Vab) / 3, I = –Ia

This explains why MHO(CG) performs well in Fig. 22. The relay location lags the fault-loop location by 30 degrees, and a BC fault was being simulated. If we assume there is no standing V0 at the relay location (ideal), there is no difference between MHO(BC)$_{COMP}$ and MHO(CG) for this fault.

It is important to note that using a MHO(PG) relay to find the performance of the MHO(PP)$_{COMP}$ is only valid for faults through a transformer with no standing zero-sequence voltage present at the relay location. For ground faults without a transformer between the relay and the fault, the zero-sequence voltage seen at the relay location will be removed by the MHO(PP)$_{COMP}$ relay and will make it underreach the MHO(PG) relay for all ground faults.

The arc-resistance coverage of the PPCOMP compared to the MHO(PP)$_{COMP}$ relay would depend on the MHO(PP)$_{COMP}$ polarization. If self-polarization is used, the PPCOMP will provide better arc-resistance coverage. Otherwise, a MHO(PP)$_{COMP}$ relay could provide better arc-resistance coverage in high forward-load conditions.

5) DY1/DY11 Transformer DLG Fault

Fig. 27 shows the phase and sequence quantities we will see on each side of the transformer. What appears to be a BCG fault on the wye side of the transformer looks unlike any standard fault type on the delta side.

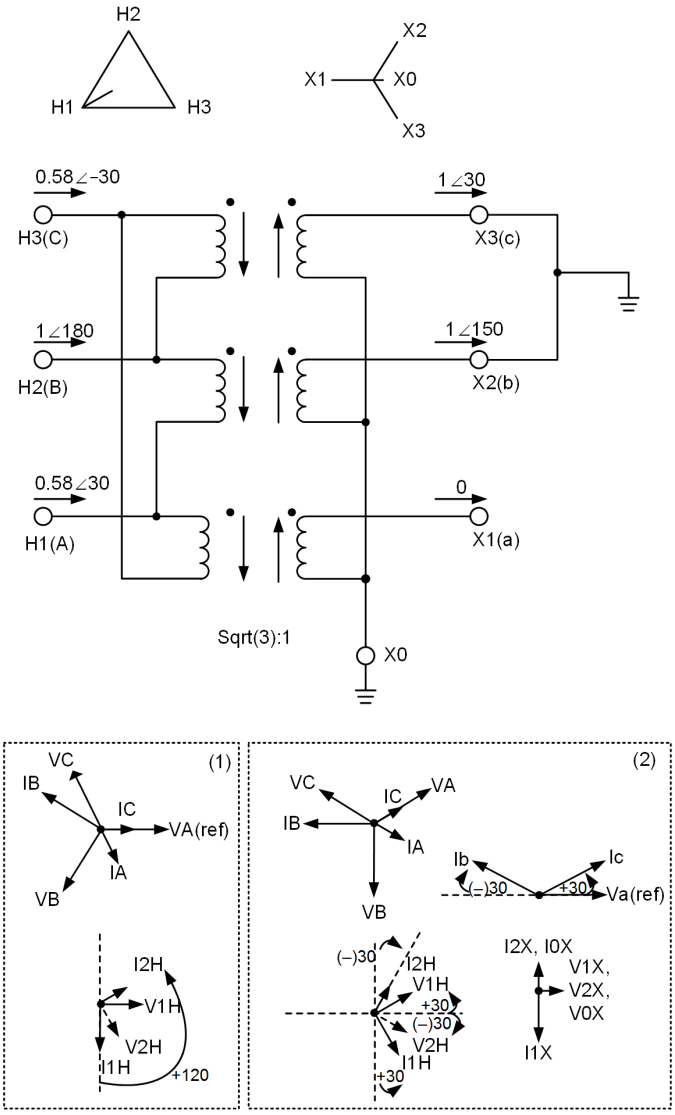

Fig. 27. DY1 Transformer – Wye-Side BCG Fault

We can define the sequence network connections when analyzing PPG faults through a delta-wye transformer in a two-source system. This is shown in Fig. 28.

Using the same parameters as defined for the PG and PP fault, we now evaluate the mho and the PPCOMP relay characteristic for a PPG fault with and without the delta-wye transformer. We start with a BCG fault, but without the phase shift introduced by the transformer. This is shown in Fig. 29.

Although the ZBG and ZCG fault loops appear to measure accurate impedance to the BCG fault in Fig. 29, [9] shows that the MHO(BG) relay will overreach if fault resistance is introduced. Therefore, MHO(PG) relays must be blocked for PPG faults without a delta-wye transformer.

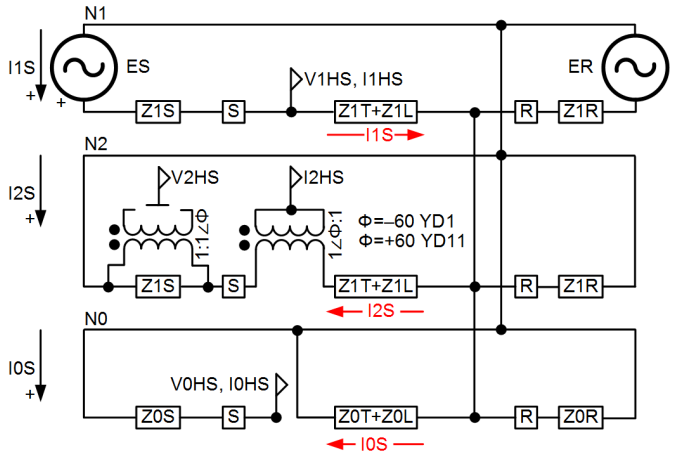

Fig. 28. Sequence Network Connections for Phase-to-Phase-to-Ground Fault Through Delta-Wye Transformer

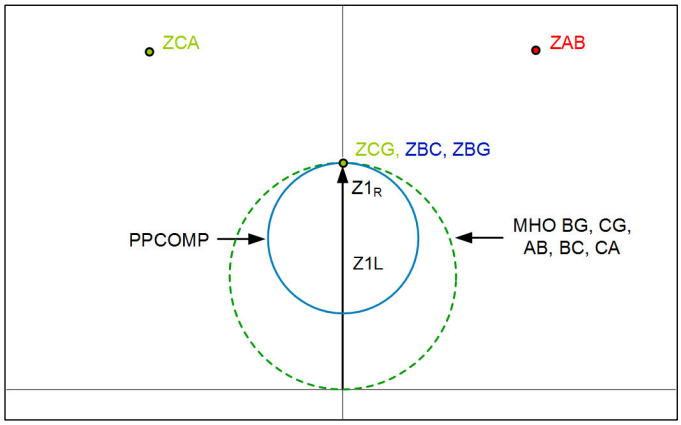

Fig. 29. Measured Fault-Loop Impedances for a BCG Fault With No Transformer Between the Relay and the Fault

Next we show the result for a DY1 transformer (Fig. 30) and a DY11 transformer (Fig. 31).

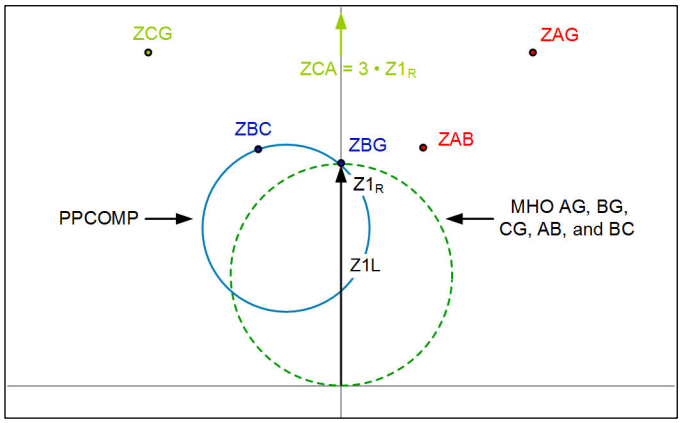

Fig. 30. Measured Fault-Loop Impedances With DY1 Transformer for a BCG Fault

From Fig. 30 and Fig. 31, we see that the MHO(PP)$_{COMP}$ relay performs just as well for a BCG fault as it did for a BC fault, which confirms it is a valid choice for reaching through a delta-wye transformer. For the DY1 transformer, ZBG is equivalent to ZBC$_{COMP}$; for the DY11 transformer, ZCG is equivalent to ZBC$_{COMP}$. Because ZBC$_{COMP}$ represents a phase-to-phase fault loop on the wye side of the transformer, there is no risk of overreach if there is fault resistance. However, we recognize an issue with the PPCOMP (solid blue line) relay for close-in PPG faults: it will NOT operate. A MHO(PP)$_{COMP}$ will not have this issue because its characteristic extends back to the origin.

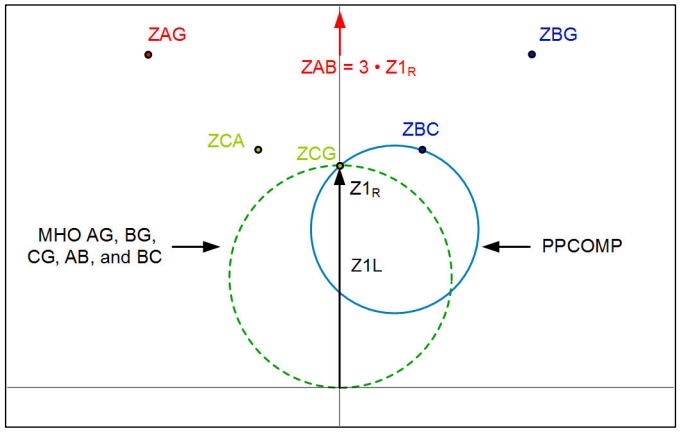

Fig. 31. Measured Fault-Loop Impedances With DY11 Transformer for a BCG Fault

It is possible to get the PPCOMP to respond to close-in faults; however, the reach must counterintuitively be pulled back, which matches our findings from the case study event in Section II. To illustrate this, we simulate a fault at 10 percent of the desired reach (0.1 ∠90 ohms) and plot the maximum allowable reach that still allows the PPCOMP to operate. For an infinitely strong system (ZS = 0), a reach of less than 0.33 ohms will allow the PPCOMP to pick up for a fault at 0.1 ohms. However, this will reduce the reach for PP faults and is not acceptable. From Fig. 32, we can see that as the source becomes weaker, the maximum allowable reach increases. Essentially, the weaker the source becomes, the greater likelihood of tripping for a close-in PPG fault with the PPCOMP relay.

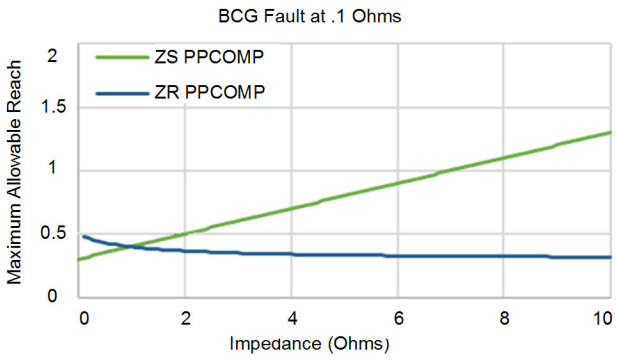

Fig. 32. Maximum Allowable Reach to Detect Close-In (10% of Reach) PPG Fault With PPCOMP Relay

It should be noted that the ratio Z1/Z0 plays an important factor in the reliability for close-in PPG faults with the PPCOMP (in Fig. 32 Z1/Z0 = 1). As Z0 decreases, V2 and I2 quantities will also decrease because the negative-sequence and zero-sequence networks are in parallel for a PPG fault. As Z0 gets smaller, the current divider reduces I2 available to the relay. From the perspective of the PPCOMP relay, a PPG fault

with Z0 = 0 is no different than a 3PH fault; the element will not operate. However, as Z0 increases, the PPCOMP becomes more reliable because a Z0 of infinity will look like a PP fault to a PPCOMP relay.

a) 3PCOMP PPG Fault Coverage

To address this issue in the PPCOMP relay, the 3PH unit of the relay is designed to operate for close-in PPG faults, as well as 3PH faults. This has been implemented in two different ways that the authors are aware of: the original 3PCOMP relay implementation (3PCOMP(OLD)) [5] and a digital relay implementation (3PCOMP(NEW)) [6]. The operating equation for the 3PCOMP(OLD) implementation is shown in (18) and (19), and the 3PCOMP(NEW) is shown in (20) and (21).

$$\begin{aligned} Sl_{3PCOMP(OLD)} &= V_{AB} - (I_A - 3 \bullet I_0) \bullet 1.5 \bullet Z1R \\ S2_{3PCOMP(OLD)} &= V_{BC(MEM)} \end{aligned} \tag{18}$$

$$3PCOMP(OLD)_{TORQUE} = IM(Sl_{3PCOMP(OLD)} \bullet S2^{*}_{3PCOMP(OLD)}) \tag{19}$$

$$\begin{aligned} Sl_{3PCOMP(NEW)} &= V_{AB} - I_{AB} \bullet Z1R \\ S2_{3PCOMP(NEW)} &= -j \bullet V_{AB} - k \bullet V_{C(mem)} \end{aligned} \tag{20}$$

$$3PCOMP(NEW)_{TORQUE} = IM(Sl_{3PCOMP(NEW)} \bullet S2^{*}_{3PCOMP(NEW)}) \tag{21}$$

From these torque definitions, it is apparent that the 3PCOMP implementations are very different. The 3PCOMP(OLD) implementation uses IA current with zero-sequence compensation. A 1.5 times multiple of relay reach is required to extend the reach correctly for 3PH faults [5]. Memory voltage must be provided because this relay must be able to respond to close-in 3PH faults. Memory voltage was implemented via a 60-cycle period resonance circuit [11]. The 3PCOMP(NEW), under careful inspection, is really a cross-polarized MHO(AB) relay written in a format consistent with the torque formula of the PPCOMP element. The K-factor allows some choice over how much memory voltage of Vc is used in the polarizing circuit. This is a factor available to the relay designer, not the relay user.

From (18) it should be apparent that ground faults involving Phase A will produce a different torque than a ground fault that does not involve Phase A because the (IA – 3 • I0) term evaluates differently. A 3PCOMP(OLD) relay will not operate for AG faults and will perform best for BCG faults for standard line protection (not reaching through a transformer). Similarly, from (19) it should be apparent that ground faults involving Phase C will produce a different torque than a ground fault that does not involve Phase C because the IAB term evaluates differently. In fact, a 3PCOMP(NEW) relay will not operate for CG faults and will perform best for ABG faults.

Both implementations of 3PCOMP can have their characteristic plotted using techniques from author Fernando Calero [12] by finding a and b from (2) in [12]; this derivation is shown in Appendix II.

We show the results of plotting the PPCOMP, 3PCOMP(OLD), and 3PCOMP(NEW) for a fault in the same system we have been using, but at a fault location of 0.33 ohms (Fig. 33 and Fig. 34). This is the point at which the PPCOMP element will drop out when set with a reach of $Z1_R = 1\angle 90$.

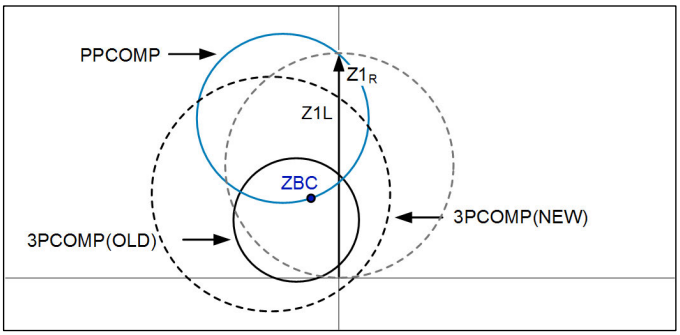

Fig. 33. BCG Fault Through a DY1 Transformer

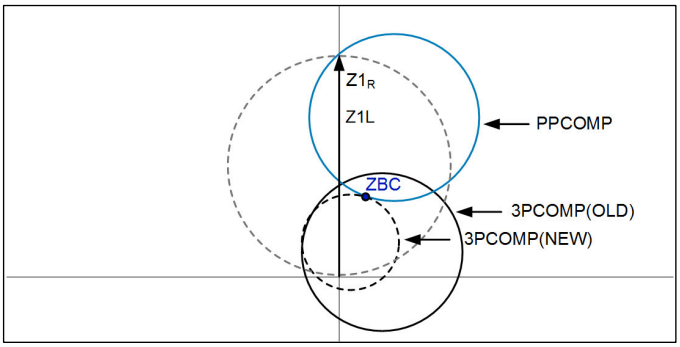

Fig. 34. BCG Fault Through a DY11 Transformer

We can see that even for this extreme case, both 3PCOMP elements will trip for this close-in BCG fault. However, we can also see that each element responds differently for the same fault through a different transformer connection. Clearly, the 3PCOMP(NEW) sees a wider range of BCG faults through a DY1 transformer than a DY11 transformer. The 3PCOMP(OLD) responds to slightly more BCG faults through a DY11 transformer than a DY1 transformer. This is an inherent issue with either 3PCOMP implementation: the relay will develop different torques depending on the faulted phases and the transformer connection if the relay is looking through a transformer.

To reduce reliance of the 3PCOMP relay for PPG faults through a transformer, care should be taken when setting the reach of the compensator relay. At the very least, we want the relay to detect close-in faults on the line, but not necessarily faults within the transformer. We can use this to our advantage because the transformer impedance moves the close-in fault location further away from relay location. In Appendix I, we derive some maximum reach considerations for the PPCOMP relay so that it can reliably detect PPG faults on the line being protected. The results of this derivation are shown in (22) and (23), where MTA is the maximum torque angle of the transformer plus line impedance.

DY Transformers

$$Z1_R < |Z1T \bullet 3| \angle MTA \tag{22}$$

YD Transformers

$$Z1_R < |2 \bullet Z1L + 3 \bullet Z1T| \angle MTA \tag{23}$$

This allows the PPCOMP relay to detect PPG faults at the transformer terminal to which the protected line is connected under worst-case conditions (infinite sources and Z1/Z0 = 1).

Technically, we may be able use a reach larger than (22) and (23); however, additional analysis would be required.

b) 3PCOMP 3PH Fault Coverage

The PPCOMP relay will not respond to 3PH faults because there is no V2 or I2 present in the system to provide operating torque. The 3PCOMP unit is used not only to detect close-in PPG faults, but also to detect 3PH faults. It should be apparent that a delta-wye transformer poses no problem with 3PH fault detection with a mho relay. Because the currents and voltages seen by the relay are a function of only positive-sequence quantities, the phase quantities will not be altered in a way that affects distance relaying. In fact, as we have shown in this section, we simply place a 60 degree phase shift in the negative-sequence network and do not touch the positive-sequence network, for simplicity.

The 3PCOMP(OLD) relay is quite interesting with regards to its performance during 3PH faults. Fig. 35 compares the 3PCOMP(NEW) and 3PCOMP(OLD) elements in a system in which Z1S = 3 ∠90, Z1L = 1 ∠90, and Z1R = 1 ∠90 with relay reach ($Z1_R$ set at 1 ∠90). A 3PH fault is placed at 1 ∠90.

The 3PCOMP(OLD) begins to overreach for 3PH faults with a load in the forward direction. The amount of overreach increases as the source becomes weaker and/or the load becomes larger. In this simple example, the reach would need to be set below 0.81 ohms to prevent an overreach for a 1 ohm fault with σ = 30. The 3PCOMP(OLD) begins to underreach for load flow in the reverse direction. In this example system, the reach would need to be set at 1.19 or higher to see a fault at 1 ohm with σ = 30. It should be noted that the exact design of the 3PCOMP(OLD) is not fully known. This example shows how a digital relay implementation of the 3PCOMP(OLD) would perform. It is reasonable to expect the original 3PCOMP(OLD) would perform similarly; however, it is not known with certainty.

The 3PCOMP(NEW) implementation is essentially a cross-polarized mho element. There is significantly less risk of overreach during load conditions [13], which is shown in Fig. 35.

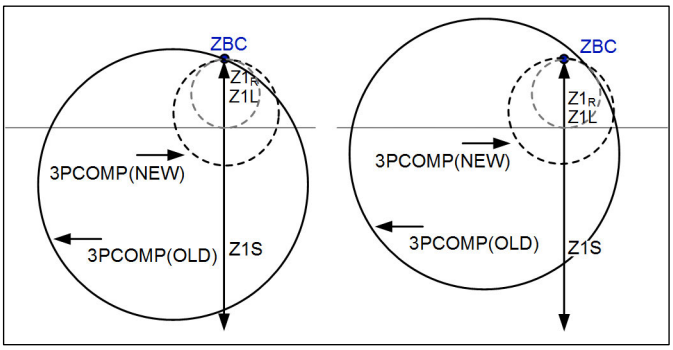

Fig. 35. 3PCOMP(NEW) and 3PCOMP(OLD) for σ = 0 on the Left and σ = 30 on the Right

B. Summary

Table I provides a review of which phase and ground relays perform best for all fault types, without a transformer, and through DY1 and DY11 transformers. The relay is on the delta side and the fault loop in question is located on the wye side when a transformer is considered. Relays listed in bold italics are not dependable for the specified fault type, even though they can respond. Other relays listed in normal text will adequately perform for the specified fault type. For PG and close-in (CI) PPG faults, the 3PCOMP method that develops the most torque is listed. The table considers ZS = 0 and no-load conditions.

TABLE I
EVALUATIONS OF BEST-PERFORMING FAULT LOOPS FOR VARIOUS FAULT TYPES THOUGH DY1 AND DY11 TRANSFORMERS

ZS = 0, No Load	**No Transformer**		**DY1**		**DY11**	
Fault	**Best Ground**	**Best Phase**	**Best Ground***	**Best Phase**	**Best Ground***	**Best Phase**
AG	AG		***MHO (AG, CG)***	***MHO(CA), PPCOMP, 3PCOMP(OLD)***	***MHO (AG, BG)***	***MHO(AB), PPCOMP, 3PCOMP(NEW)***
BG	BG		***MHO (AG, BG)***	***MHO(AB), PPCOMP, 3PCOMP(NEW)***	***MHO (BG, CG)***	***MHO(BC), PPCOMP, 3PCOMP(NEW)***
CG	CG		***MHO (BG, CG)***	***MHO(BC), PPCOMP, 3PCOMP(NEW)***	***MHO (AG, CG)***	***MHO(CA), PPCOMP, 3PCOMP(OLD)***
AB		MHO(AB)/PPCOMP	MHO(AG)	MHO(AB)COMP/PPCOMP	MHO(BG)	MHO(AB)COMP/PPCOMP
BC		MHO(BC)/PPCOMP	MHO(BG)	MHO(BC)COMP/PPCOMP	MHO(CG)	MHO(BC)COMP/PPCOMP
CA		MHO(CA)/PPCOMP	MHO(CG)	MHO(CA)COMP/PPCOMP	MHO(AG)	MHO(CA)COMP/PPCOMP
ABG (CI)		MHO(AB)/3PCOMP(NEW)	MHO(AG)	MHO(AB)COMP/ 3PCOMP(NEW)	MHO(BG)	MHO(AB)COMP/ 3PCOMP(NEW)
BCG (CI)		MHO(BC)/3PCOMP(OLD)	MHO(BG)	MHO(BC)COMP/ 3PCOMP(NEW)	MHO(CG)	MHO(BC)COMP/ 3PCOMP(OLD)
CAG (CI)		MHO(CA)/ 3PCOMP(OLD/NEW)	MHO(CG)	MHO(CA)COMP/ 3PCOMP(OLD)	MHO(AG)	MHO(CA)COMP/ 3PCOMP(NEW)

* = Blocked from operating; illustration purposes only

V. Revisit Case Study With Dynamic Characteristic

Armed with the dynamic characteristic derived in Section III and the general information discussed in Section IV, we revisit the event report introduced in Section II and plot the key characteristics at a point in the event in which the $PPCOM_{TORQUE}$ was the most positive (underreaching).

A. Plot the Relay Characteristics

We recognized early that reducing the reach increased the dependability of the PPCOMP; we now include both 3PCOMP relays for evaluation to determine if they will help maintain a trip signal. Further, we include a positive-sequence polarized MHO(BC) element because it was recognized early in our analysis that this element would have also been dependable. To declutter the plots in the impedance plane, we only consider the ZBC impedance. However, we will note that a MHO(CA) would operate and provide the lowest-required reach to trip. A MHO(AB) element would not operate with the reach settings in service at the time of the fault ($Z1_R = 64\angle 86.1$). The results of this for the original relay reach are shown in Fig. 36. Recall that the compensator relay was set to trip for faults in the reverse direction, and this fault was in the reverse direction based on the CT connection polarity. This places the relay reach in the third quadrant of the complex plane rather than the first quadrant.

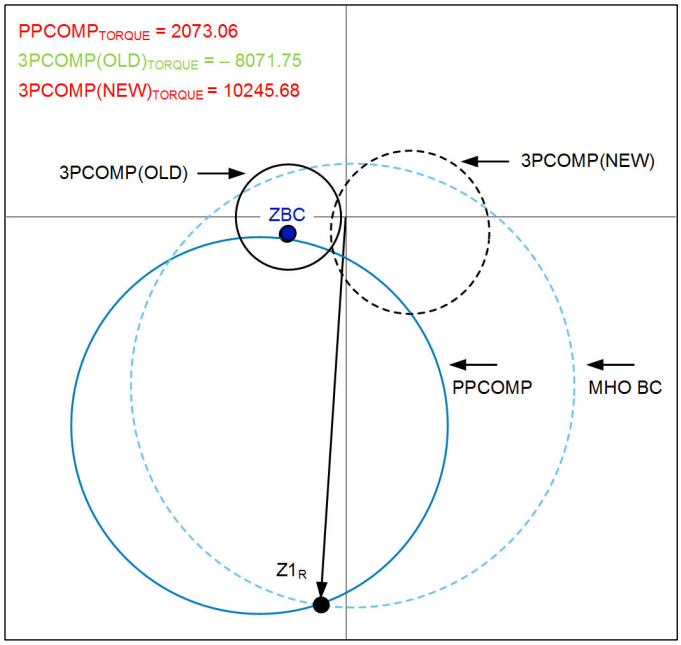

Fig. 36. Characteristic Plot for ZBC Impedance at Relay Reach = 64 Ohms

From Fig. 36 we can see that the $PPCOMP_{TORQUE}$ is positive; this is displayed graphically by ZBC positioned just outside the PPCOMP characteristic circle. The PPCOMP characteristic is offset such that the circle sees a reduction in size, rather than expansion. This can easily be seen when comparing to the positive-sequence polarized MHO(BC) characteristic, which is offset so that the circle expands. Increasing the reach of the PPCOMP relay simply moves the circle farther away from the x-axis and leads to the reduction in dependability. With ZBC on the edge of the PPCOMP circle, the small changes in fault resistance shown in Fig. 2 allowed ZBC to move in and out of the circle throughout the event and ultimately were the reason PPCOMP was not able to time out.

We can also see that 3PCOMP(NEW), which was the 3PH relay in service at the time of the fault, does not see this fault within its characteristic ($3PCOMP(NEW)_{TORQUE}$ is positive).

We can see that 3PCOMP(OLD) torque is negative; this is represented in the characteristic plot as ZBC being near the center of that characteristic circle. Interestingly, it appears that a 3PCOMP(OLD) relay would have timed out and tripped for this fault.

From our discussion in Section IV and the recommendation in (23) for a YD transformer, the maximum reach that should have been considered was 21.97 ohms. We also note that the MTA setting chosen initially should be lowered to include the effects of the transformer and line characteristic impedance angle. Fig. 37 shows the results of pulling back the reach to the maximum allowable reach from (23).

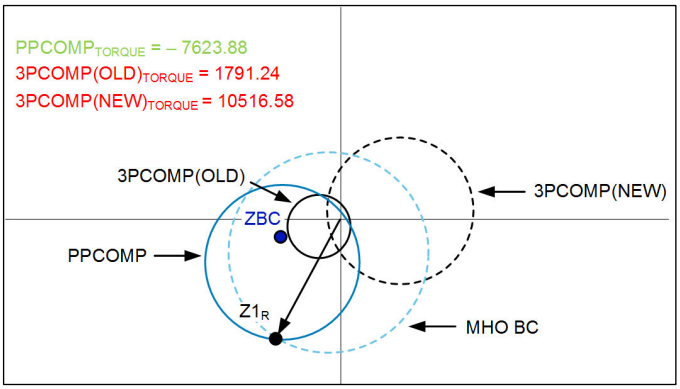

Fig. 37. Characteristic Plot for ZBC Impedance at Relay Reach = 21.97 Ohms

From Fig. 37 we can see that pulling back the reach to 21.97 ohms does two things. First, it allows the PPCOMP element to respond to the fault without issue. Second, the 3PCOMP(OLD) relay no longer calls for a trip. Pulling back the reach to increase PPCOMP dependability is counterintuitive and requires plotting of the dynamic PPCOMP characteristic to determine how the reach setting affects the performance of this relay.

B. Effects of Shunt Load Impedance

Although the only event report available on the delta side of the transformer indicates this is a Phase C-to-ground fault, the PPCOMP relay performs similarly to a BCG fault thorough a YD11 transformer. Unfortunately, not all 34.5 kV fault data, system configuration data, and load data at the time of the fault were available to analyze this further. However, there were many tapped loads on the protected line, which will act like a shunt impedance path that will draw negative-sequence current away from the relay. Conceptually, this is similar to the effect that the zero-sequence impedance has on negative-sequence current for PPG faults. Fig. 38 shows a sequence diagram for a delta-wye transformer in a radial system in which a PG fault occurs on the delta side with a shunt loads connected on the line. The relay is located on the wye side. As the load impedance reduces, the negative-sequence current available to

the relay also reduces, affecting the dependability of the PPCOMP relay. Fig. 38 also shows that the load impedance serves as the connection that permits fault current to flow through the delta-wye transformer.

Although we do not expect a PPCOMP relay to be dependable for PG faults, shunt loads have more of an influence on dependability of the PPCOMP, as compared to a MHO(PP) or MHO(PP)$_{COMP}$. Reference [9] notes that if impedances are low enough in these shunt loads, the PPCOMP will become disabled, even for PP faults.

As mentioned in Section II, it is possible that Breaker 3 of the utility was open prior to the fault. If this was the case, the resultant PG fault current seen on the utility system would have been very low after Breaker 1 opened. The fault current seen by the utility would have been limited by the shunt load impedance, and it may not have produced enough ground current to allow other 51GT relays to time out.

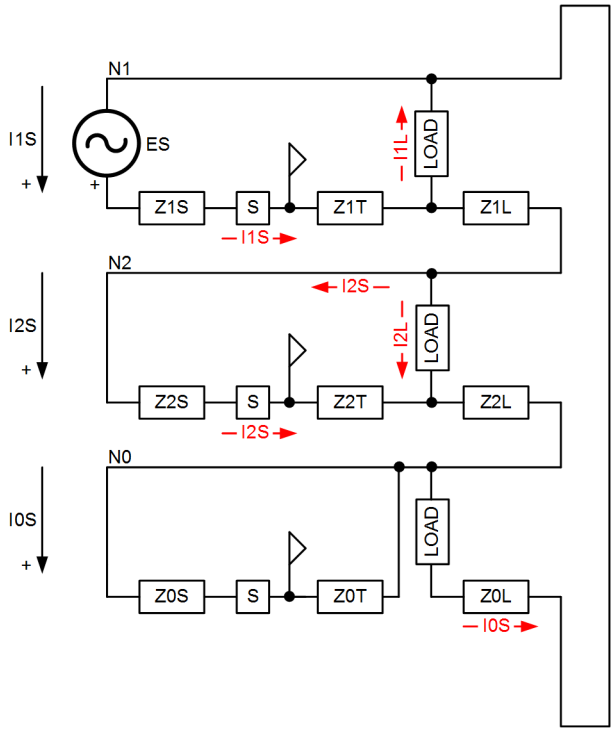

Fig. 38. Wye-Delta Transformer with PG Fault and Shunt Load

C. *Alter the Faulted Phases and Compare 3PCOMP Performance*

This section explores how the 3PCOMP relays would have responded had the fault on the delta side of the transformer been BG instead of CG. To accomplish this, we insert the phase inputs into the formulas of our characteristic plots. This is accomplished by transferring BC to AB, CA to BC, and AB to CA voltages and currents. The results of this are shown in Fig. 39 with only 3PCOMP(OLD) and 3PCOMP(NEW) plotted at the original reach setting.

From Fig. 39, we see that the 3PCOMP(NEW) would have operated had the fault on the delta side of the transformer been BG instead of CG. In fact, 3PCOMP(NEW) develops over three times more torque than 3PCOMP(OLD). While 3PCOMP(OLD) develops less torque for a BG fault over the CG fault, it still would have tripped. Even though nothing has changed other than the faulted phase, the torque of the only tripping unit available for this fault changes. This is unique to some ground faults with a compensator relay. A MHO(PP) relay, with three tripping units available for any fault, will simply see the most dependable fault loop move from CA to BC in this example. There is no difference in the reliability of a MHO(PP) relay based on the faulted phases involved.

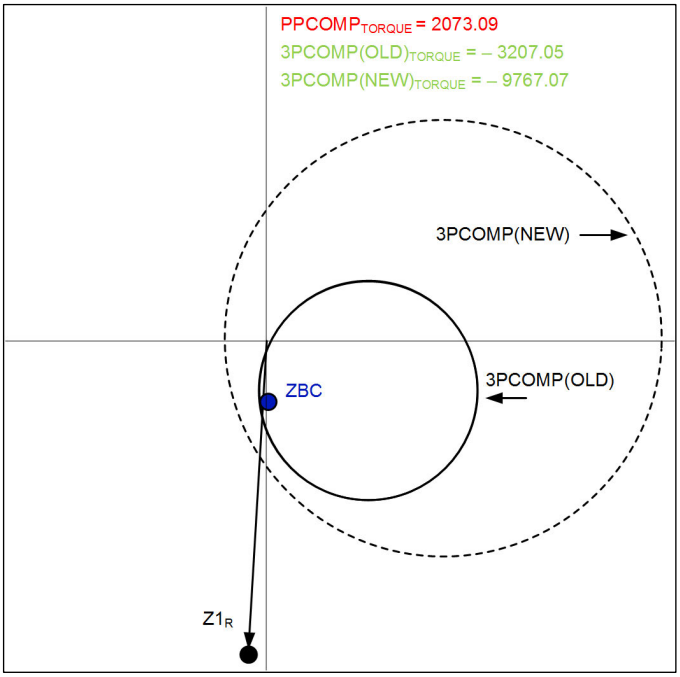

Fig. 39. ZCA Impedance From Original Event Converted to ZBC and Evaluated With Reach at Original Value

D. *Evaluate MHO(PP)$_{COMP}$ Performance*

In this section, we look at how a MHO(PP)$_{COMP}$ relay monitoring ZAB$_{COMP}$, ZBC$_{COMP}$, and ZCA$_{COMP}$ loops would have responded, because this is a viable way to protect for faults through a delta-wye transformer, as discussed in Section IV. Fig. 40 shows the results of the plotted impedances inside a self-polarized mho circle.

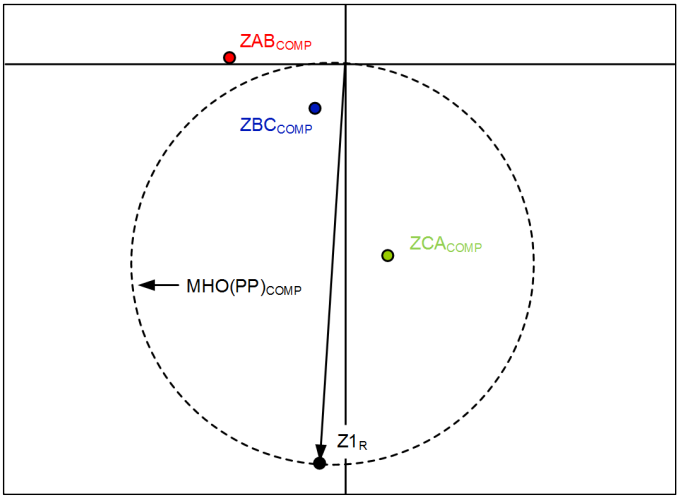

Fig. 40. MHO(PP)$_{COMP}$ Performance for Fault at Original Reach Setting

From Fig. 40, we see that the ZBC_{COMP} and ZCA_{COMP} impedance fall within the characteristic. For this fault, the $MHO(PP)_{COMP}$ relay is more dependable than a PPCOMP relay without additional reach considerations that come with using the compensator relay.

VI. Conclusions

We offer the following conclusions for this paper:

- Delta-wye transformer connections produce a phase shift in positive- and negative-sequence currents that affect the reach of distance relays looking through them.
- No distance relay is reliable enough to detect PG faults through a delta-wye or wye-delta transformer.
- Traditional MHO(PP) relays are not reliable enough to detect PP or PPG faults through a delta-wye transformer. However, they are reliable enough to detect 3PH faults through a delta-wye transformer.
- PPCOMP or $MHO(PP)_{COMP}$ relays are reliable for PP faults through a delta-wye transformer. The $MHO(PP)_{COMP}$ relay can give faulted phase indication; whereas, the PPCOMP will not.
- The PPCOMP relay can be unreliable for close-in PPG faults through a delta-wye transformer. This is particularly true if the reach is set longer than the result of (22) and (23). If the PPCOMP relay is being used to directionally torque control over current elements, understand that simply setting the relay at maximum reach is not the best practice.
- The 3PCOMP relay (both [OLD] and [NEW]) will respond to some close-in PPG faults that the PPCOMP relay missed. However, each relay will respond differently depending on the phases involved in the fault. Table I shows the best-performing elements.
- A $MHO(PP)_{COMP}$ element is reliable for close-in PPG faults through a delta-wye transformer. No additional considerations are required related to the reach (it can be set rather long without any negative effects). Further, the dependability of the $MHO(PP)_{COMP}$ element does not change based on the phases involved in the fault.
- The 3PCOMP(NEW) relay is more secure than 3PCOMP(OLD) for a forward load during a 3PH fault (Fig. 36).
- The PPCOMP relay is more affected by load conditions than positive-sequence memory-polarized mho relays for faults. The PPCOMP will lose more fault resistance coverage than a V1 memory-polarized MHO(PP) relay for load in the forward direction (Fig. 7). Additionally, if there are shunt loads on the protected line, the PPCOMP relay will see a decrease in dependability for all fault types.
- A MHO(PP) distance relay and a compensator distance relay respond differently for PP faults under load conditions and ground faults (PG and PPG) regardless of loading conditions. It is not appropriate to attempt coordination between a MHO(PP) relay and a compensator distance relay.
- Multiple solutions can prevent the miscoordination problem that arose in this event, including:
  - Use a 67 and/or directional 51 relay to coordinate with the tie. This allows for the coordination of similar relay types and does not require complicated studies.
  - Set the PPCOMP according to the guidelines defined in (23). This will shorten the PPCOMP reach and allow it to be more dependable. However, the PPCOMP will suffer a reduced fault resistance coverage.
  - Use $MHO(PP)_{COMP}$ relays to reach through a delta-wye transformer. For the relay in service at the time, this option was not available.
  - Use MHO(PP) elements to reach through a delta-wye transformer. In this installation, the intent was to detect any fault on the delta side of the transformer; therefore, even though a MHO(PP) is not acceptable to ensure an exact reach point, it is acceptable to detect faults. With the relays in service at the time of the fault, the relay would need to be told it had wye PTs connected (even though they are open delta), so that MHO(PP) elements could be used. This would have the negative side effect of making the relay unreliable for many metering quantiles, including power.
  - Take care that the tie does not have a farther reach than the applied distance relay on the main. To confirm, a fault study would be required, comparing the torques of the selected distance element and verifying it operates for all tie overcurrent conditions. However, we can never ensure coordination between dissimilar elements because changes in the system will affect distance and overcurrent elements differently.

VII. Appendix I

In this Appendix we intend to find the maximum reach for a PPCOMP relay that can still detect a PPG fault at the transformer terminals.

First, we examine a YD transformer. Because we are looking at the performance of the PPCOMP relay, we are not concerned with phase shifts in the negative-sequence network; therefore, the transformers were removed. In the network shown in Fig. 41, k defines the ZT pu impedance on a base of ZT + ZL.

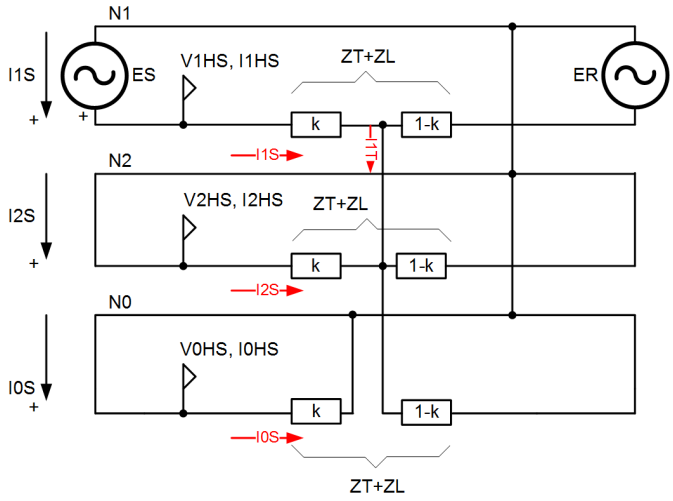

Fig. 41. Simplified Sequence Network Connections for PPG Fault Through a Wye-Delta Transformer

Recall that the PPCOMP relay is simply a line-drop compensated V1/V2 balance relay as defined by (5).

Our goal is to find the largest Z1R for which the relay can still trip for a fault at k. We can reorganize (5) to the simplification in (24) and (25), by assuming we are dealing with an infinite voltage source of 1 pu; we are only considering a bolted fault and no fault resistance. Under these assumptions, there are two conditions in which a balance condition is met:

$$\frac{1}{(|I1_{S(pu)}|+|I2_{S(pu)}|)}=Z1_{R(MIN)} \tag{24}$$

$$\frac{1}{(|I1_{S(pu)}|-|I2_{S(pu)}|)}=Z1_{R(MAX)} \tag{25}$$

From this we can see that a PP fault in which $|I1_R| = |I2_R|$ has an infinite maximum reach to detect a fault. So, PP faults do not suffer from a maximum reach issue. The minimum reach required to detect the fault is simply "the reach." However, for PPG faults, the smaller $|I2_R|$ becomes, the smaller $Z1_{R(MAX)}$ also becomes. We see a smaller $|I2_R|$ when Z0 is small for PPG faults. In our example, we consider Z1 = Z0 and infinite sources. We want to relate $Z1_{R(MAX)}$ to the ZT and ZL parameters. The following example is a derivation of that.

$$I1_{T(PU)}=\frac{1}{k\bullet(1-k)+\frac{k\bullet(1-k)\bullet(1-k)}{k\bullet(1-k)+(1-k)}}$$

$$I1_{T(PU)}=\frac{1}{\frac{k\bullet(1-k)(2+k)}{(1+k)}}$$

$$I1(\text{Current Divider})=\frac{1-k}{k+(1-k)}$$

$$I1(\text{Current Divider})=1-k$$

$$I1_{S(PU)}=\frac{(1-k)}{\frac{k\bullet(1-k)(2+k)}{(1+k)}}$$

$$I1_{S(PU)}=\frac{(1+k)}{k\bullet(2+k)}$$

$$I2(\text{Current Divider})=\frac{(1-k)}{k\bullet(1-k)+(1-k)}$$

$$I2(\text{Current Divider})=\frac{1}{(1+k)}$$

$$I2_{S(PU)}=\frac{(1+k)}{k\bullet(2+k)}\bullet\frac{1}{(1+k)}$$

$$I2_{S(PU)}=\frac{1}{k\bullet(2+k)}$$

$$I1_{S(PU)}-I2_{S(PU)}=\frac{(1+k)}{k\bullet(2+k)}-\frac{1}{k\bullet(2+k)}=\frac{k}{k\bullet(2+k)}$$

$$Z1_{R(MAX)(PU)}=\frac{1}{\frac{k}{k\bullet(2+k)}}=2+k$$

$$Z1_{R(MAX)}=\left(2+\frac{ZT}{ZT+ZL}\right)\bullet(ZT+ZL)$$

$$Z1_{R(MAX)}=3\bullet ZT+2\bullet ZL$$

It can also be seen that if we use (24) to find the minimum required relay reach, the result will be simply ZT + ZL, which is as expected.

Next we look at how to determine the maximum reach for a DY transformer. We note that the zero-sequence network changes, which has an influence on (5). Fig. 42 shows the network connections.

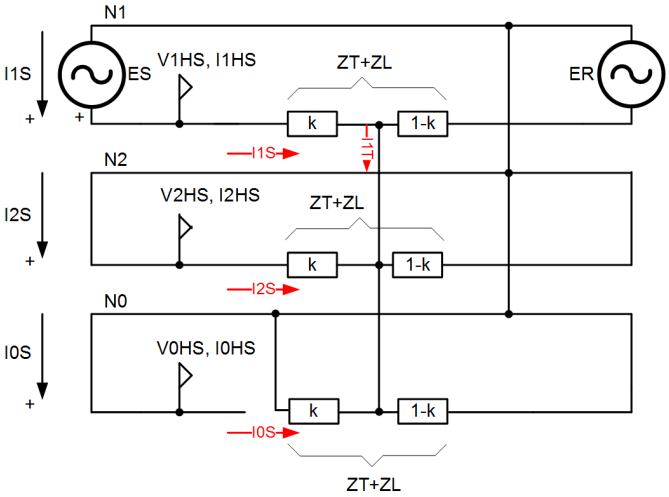

Fig. 42. Simplified Sequence Network Connections for PPG Fault Through a Delta-Wye Transformer

We want to relate $Z1_{R(MAX)}$ to the ZT and ZL parameters. The following example is a derivation of that.

$$I1_{T(PU)} = \frac{1}{k \bullet (1-k) + \frac{k \bullet (1-k) \bullet k \bullet (1-k)}{k \bullet (1-k) + k \bullet (1-k)}}$$

$$I1_{T(PU)} = \frac{1}{k \bullet (1-k) \bullet (1+.5)}$$

$$I1(\text{Current Divider}) = \frac{(1-k)}{k + (1-k)}$$

$$I1(\text{Current Divider}) = 1-k$$

$$I1_{S(PU)} = \frac{1}{1.5 \bullet k}$$

$$I2(\text{Current Divider}) = \frac{k \bullet (1-k)}{k \bullet (1-k) + k \bullet (1-k)}$$

$$I2(\text{Current Divider}) = .5$$

$$I2_{S(PU)} = \frac{1}{1.5 \bullet k} \bullet .5$$

$$I2_{S(PU)} = \frac{1}{3 \bullet k}$$

$$I1_{S(PU)} - I2_{S(PU)} = \frac{1}{1.5 \bullet k} - \frac{1}{3 \bullet k} = \frac{1}{3 \bullet k}$$

$$Z1_{R(MAX)(PU)} = \frac{1}{\frac{1}{3 \bullet k}} = 3 \bullet k$$

$$Z1_{R(MAX)} = \left(3 \bullet \frac{ZT}{ZT + ZL}\right) \bullet (ZT + ZL)$$

$$Z1_{R(MAX)} = 3 \bullet ZT$$

It can also be seen that if we use (24) to find the minimum required relay reach, the result will be simply ZT + ZL, which is as expected.

VIII. Appendix II

Both implementations of 3PCOMP can have their characteristic plotted using techniques from Calero [12] by finding "a" and "b" from (2) in [12]. The "a" number is typically the reach setting of the distance element; whereas, "b" typically represents the expansion on the distance element. The midpoint of a line that connects the "a" and "b" coordinates represents the center point of the distance element circle.

We start with 3PCOMP(OLD); the torque equations are shown here:

$$S1_{3PCOMP(OLD)} = VAB - (IA - I0) \bullet 1.5 \bullet Z1R$$

$$S2_{3PCOMP(OLD)} = VBC$$

$$3PCOMP(OLD)_{TORQUE} = IM(S1_{3PCOMP(OLD)} * \text{conj}(S2_{3PCOMP(OLD)}))$$

From [12], we first need to convert the torque evaluation from using an imaginary operator to a using a real operator. We do this by shifting $S2_{3PCOMP(OLD)}$ by 90 degrees, which allows the torque evaluation to be equivalent to its original value.

$$S2C_{3PCOMP(OLD)} = jVBC$$

$$3PCOMP(OLD)_{TORQUE} = RE(S1_{3PCOMP(OLD)} * \text{conj}(S2C_{3PCOMP(OLD)}))$$

Next, we divide $S1_{3PCOMP(OLD)}$ and $S2_{C3PCOMP(OLD)}$ by IAB because it allows us to easily develop a reference to the ZAB loop.

$$\frac{S1_{3PCOMP(OLD)}}{IAB} = ZAB - \frac{IA - I0}{IAB} \bullet 1.5 \bullet Z1R$$

$$\frac{S2C_{3PCOMp(OLD)}}{IAB} = ZAB + \frac{jVBC}{IAB} - ZAB$$

$$a_{AB} = \frac{IA - I0}{IAB} \bullet 1.5 \bullet Z1R$$

$$b_{AB} = -\left(\frac{jVBC}{IAB} - ZAB\right)$$

The a_{AB} and b_{AB} points represent two points on the circle in the ZAB plane for which a circle can be defined. If we want to convert to the ZBC plane, we can perform a conversion:

$$\frac{S1_{3PCOMP(OLD)}}{IAB} = \left(ZAB - \frac{IA - I0}{IAB} \bullet 1.5 \bullet Z1R\right) \bullet \frac{ZBC}{ZAB}$$

$$\frac{S2C_{3PCOMp(OLD)}}{IAB} = \left(ZAB + \frac{jVBC}{IAB} - ZAB\right) \bullet \frac{ZBC}{ZAB}$$

$$a_{BC} = \left(\frac{IA - I0}{IAB} \bullet 1.5 \bullet Z1R\right) \bullet \frac{ZBC}{ZAB}$$

$$b_{BC} = -\left(\frac{jVBC}{IAB} - ZAB\right) \bullet \frac{ZBC}{ZAB}$$

The a_{BC} and b_{BC} points represent two points on the circle in the ZBC plane for which a circle can be defined. This allows us to plot the response of 3PCOMP(OLD) in the ZBC plane.

Then, we go through the same exercise for 3PCOMP(NEW) by starting with the original torque equations.

$$S1_{3PCOMP(NEW)} = V_{AB} - I_{AB} \bullet Z1R$$

$$S2_{3PCOMP(NEW)} = -j \bullet V_{AB} - k \bullet V_{C(mem)}$$

$$3PCOMP(NEW)_{TORQUE} = IM(S1_{3PCOMP(NEW)} \bullet S2_{3PCOMP(NEW)}^{*})$$

We then shift $S2_{3PCOMP(new)}$ by 90 degrees, which allows the torque evaluation to be equivalent to its original value.

$$S2C_{3PCOMP(NEW)} = V_{AB} - j \bullet (k \bullet V_{C(mem)})$$

$$3PCOMP(NEW)_{TORQUE} = RE(S1_{3PCOMP(NEW)} \bullet S2C_{3PCOMP(NEW)}^{*})$$

Next, we divide $S1_{3PCOMP(NEW)}$ and $S2_{C3PCOMP(NEW)}$ by IAB because it allows us to easily develop a reference to the ZAB loop.

$$\frac{S1_{3PCOMP(NEW)}}{IAB} = ZAB - Z1R$$

$$\frac{S2C_{3PCOMP(NEW)}}{IAB} = ZAB + \frac{V_{AB} - j \bullet (k \bullet V_{C(mem)})}{IAB} - ZAB$$

$$a_{AB} = Z1R$$

$$b_{AB} = -\left(\frac{-j \bullet (k \bullet V_{C(mem)})}{IAB}\right)$$

The a_{AB} and b_{AB} points represent two points on the circle in the ZAB plane for which a circle can be defined. If we want to convert to the ZBC plane, we can perform a conversion:

$$\frac{S1_{3PCOMP(NEW)}}{IAB} = (ZAB - Z1R) \bullet \frac{ZBC}{ZAB}$$

$$\frac{S2C_{3PCOMP(NEW)}}{IAB} = \left(ZAB + \frac{V_{AB} - j \bullet (k \bullet V_{C(mem)})}{IAB} - ZAB \right) \bullet \frac{ZBC}{ZAB}$$

$$a_{BC} = Z1R \bullet \frac{ZBC}{ZAB}$$

$$b_{BC} = -\left(\frac{-j \bullet (k \bullet V_{C(mem)})}{IAB} \right) \bullet \frac{ZBC}{ZAB}$$

The a_{BC} and b_{BC} points represent two points on the circle in the ZBC plane for which a circle can be defined. This allows us to plot the response of 3PCOMP(NEW) in the ZBC plane.

IX. Acknowledgment

The authors greatly appreciate the help of Don Fentie for his outstanding work in helping us plot the characteristics shown in this paper. His work was invaluable in helping us find a way to visualize the compensator characteristic. Additionally, the authors thank Ram Palaniappan for his advice on various figures throughout the paper.

X. References

[1] D. Costello, M. Moon, and G. Bow, "Use of Directional Elements at the Utility-Industrial Interface," proceedings of the 31st Annual Western Protective Relay Conference, Spokane, WA, October 2004.

[2] K. Zimmerman and D. Roth, "Evaluation of Distance and Directional Relay Elements on Lines With Power Transformers or Open-Delta VTs," proceedings of the 32nd Annual Western Protective Relay Conference, Spokane, WA, October 2005.

[3] J. Mooney and J. Peer, "Application Guidelines for Ground Fault Protection," proceedings of the 24th Annual Western Protective Relay Conference, Spokane, WA, October 1997.

[4] D. D. Fentie, "Understanding the Dynamic Mho Distance Characteristic," proceedings of the 42nd Annual Western Protective Relay Conference, Spokane, WA, October 2015.

[5] W. K. Sonnemann and H. W. Lenser, "Compensator Distance Relaying Part I," *AIEE Transactions,* Vol. 77, Part III, June 1958, pp. 372–382.

[6] J. Larson and R. McDaniel, "Man-Made Faults – Line Protection Operation for an Unintended Phase Cross-Connect Condition," proceedings of the 42nd Annual Western Protective Relay Conference, Spokane, WA, October 2015.

[7] G. Benmouyal, N. Fischer, and B. Smith, "Performance Comparison Between Mho Elements and Incremental Quantity-Based Distance Elements," proceedings of the 43rd Annual Western Protective Relay Conference, Spokane, WA, October 2016.

[8] J. M. Crockett and W.A. Elmore, "Performance of Phase-to-Phase Distance Units," proceedings of the 13th Annual Western Protective Relay Conference, Spokane, WA, October 1986.

[9] D. Costello and K. Zimmerman, "Determining the Faulted Phase," proceedings of the 36th Annual Western Protective Relay Conference, Spokane, WA, October 2009.

[10] GE Protection and Control, "GEK-26420B: Offset Mho Distance Relay Type CEB51B Instructions*."*

[11] W. E. Rich and H. J. Calhoun, "Compensator Distance Relaying Part II," *AIEE Transactions,* Vol. 77, Part III, June 1958, pp. 383–387.

[12] F. Calero, "Distance Elements: Linking Theory With Testing," proceedings of the 35th Annual Protective Relay Conference, Spokane, WA, October 2008.

[13] J. Roberts, A. Guzman, and E. O. Schweitzer, III, "Z = V/I Does Not Make a Distance Relay," proceedings of the 20th Annual Western Protective Relay Conference, Spokane, WA, October 1993.

XI. Biographies

Dustin Hohenbery is a facility engineer for Caterpillar Global Facilities. He received his bachelor's degree in Electrical Engineering from Bradley University. His present job responsibilities include maintaining the power distribution equipment for the Caterpillar East Peoria facility and designing of new electrical equipment installs around the central Illinois area.

Ryan McDaniel earned his B.S. in Computer Engineering from Ohio Northern University in 2002. In 1999, Ryan was hired by American Electric Power (AEP) as a relay technician, where he commissioned protective systems. In 2002, Ryan began working in the Station Projects Engineering group as a protection and control engineer. His responsibilities in this position included protection and control design for substation, distribution, and transmission equipment as well as coordination studies for the AEP system. In 2005, Ryan joined Schweitzer Engineering Laboratories, Inc. (SEL) and is currently a senior field application engineer. His responsibilities include providing application support and technical training for protective relay users. Ryan is a registered professional engineer in the state of Illinois and a member of IEEE.

Harish Chaluvadi received his B.T. degree in Electrical and Electronics Engineering from National Institute of Technology, Tiruchirappalli, India, in 2005, and his M.S. in Electrical Engineering from Clemson University in 2008. He has over 10 years of experience in power system engineering including analytical studies, design, field testing, and project management. He joined SEL Engineering Services, Inc. (SEL ES) in Lake Zurich, IL, in 2012 as a Project Engineer. He is a licensed professional engineer in the states of California, Iowa, Wisconsin, and Minnesota.

Michael J. Thompson received his B.S., magna cum laude, from Bradley University in 1981 and an M.B.A. from Eastern Illinois University in 1991. Upon graduating, he served nearly 15 years at Central Illinois Public Service (now AMEREN). Prior to joining Schweitzer Engineering Laboratories, Inc. (SEL) in 2001, he was involved in the development of several numerical protective relays while working at Basler Electric. He is presently a Fellow Engineer with SEL Engineering Services, Inc. (SEL ES). He is a senior member of the IEEE, officer of the IEEE Power & Energy Society (PES) Power System Relaying and Control Committee (PSRCC), past chairman of the Substation Protection Subcommittee of the PSRCC, and recipient of the Standards Medallion from the IEEE Standards Association in 2016. Michael is a registered professional engineer in six jurisdictions, was a contributor to the reference book *Modern Solutions for the Protection, Control, and Monitoring of Electric Power Systems*, has published numerous technical papers and magazine articles, and holds three patents associated with power system protection and control.

© 2019 by Caterpillar and
Schweitzer Engineering Laboratories, Inc.
All rights reserved.
20190402 • TP6894-01